EMU
Journal of
Pharmaceutical
Sciences

ISSN: 2651-3587
Volume 3 / Issue 1

EMUJPharmSci

March 2020

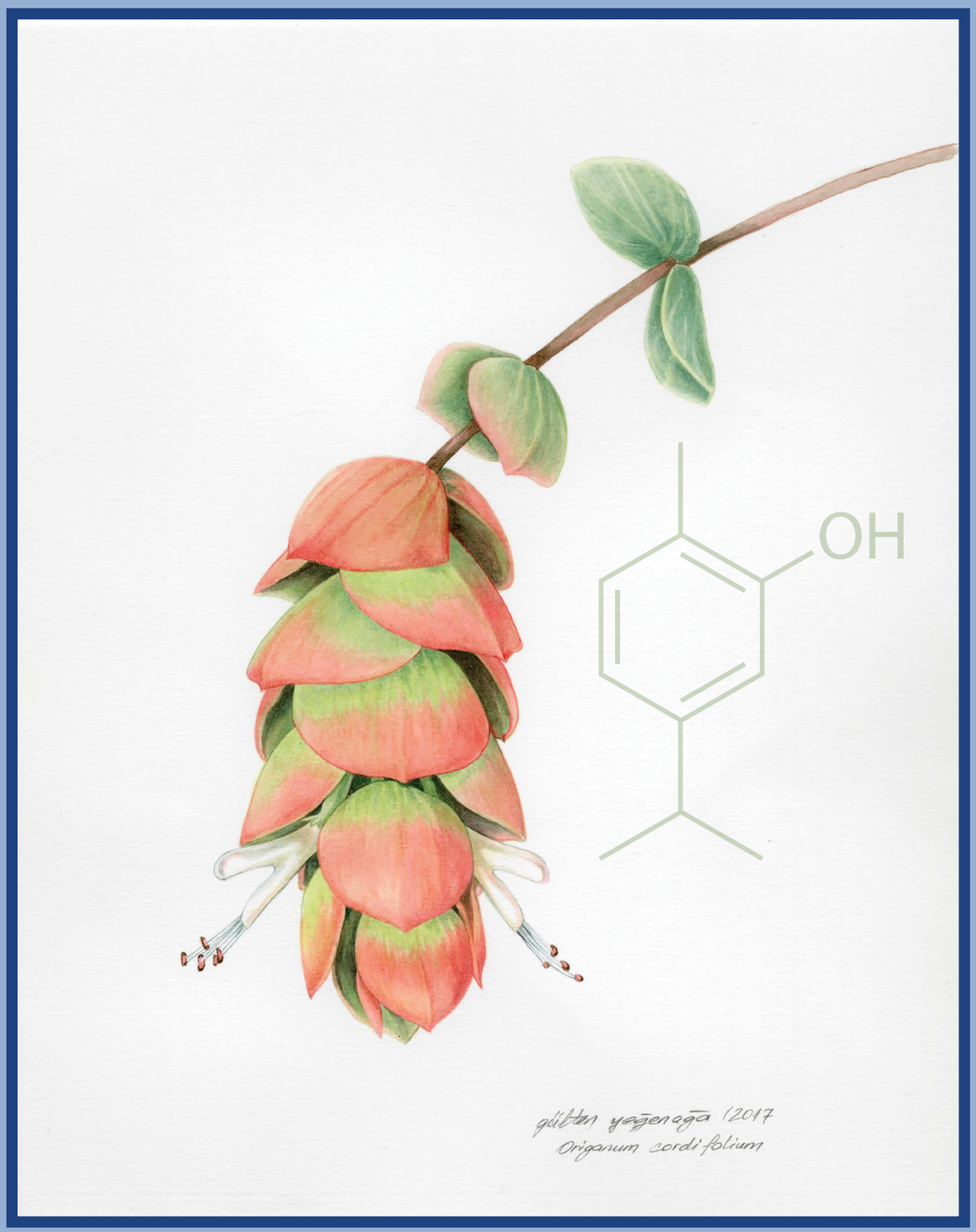

Eastern Mediterranean University Press

EMU
Journal of
Pharmaceutical
Sciences

EMUJPharmSci

Origanum cordifolium* **in cover picture was illustrated by Gülten Yeğenağa

EMU Journal of Pharmaceutical Sciences

EMUJPharmSci

Advisory/Scientific Board

EMU Journal of Pharmaceutical Sciences
EMUJPharmSci

GUIDE FOR AUTHORS

EMU Journal of Pharmaceutical Sciences (EMUJPharmSci) covers the research on all aspects of Pharmacy presented as original articles, short reports and reviews.

EMU Journal of Pharmaceutical Sciences is published three times (March, August, December) in a year. It is an open access and peer-reviewed journal.

- Contributions to EMU Journal of Pharmaceutical Sciences must be in English.
- All manuscripts are subject to editorial review.
- The manuscripts should not be previously published or accepted for publication and should not be submitted or under simultaneous consideration for publication elsewhere.
- The manuscripts are published in the order of final acceptance after review and revision.
- If the manuscript is returned to authors for revision and the revised manuscript is not received by the editor within 2 months it will be treated as a new article.
- If the manuscript is accepted and the proof is returned to the authors, corrected proofs should be sent to the editor within 5 days.

Original articles: These are limited to 15 typewritten pages in addition to supplementary materials (schemes, tables, figures, etc.).

Short papers: Short papers are limited to 5 typewritten pages and maximum of 2 supplementary materials (schemes, tables, figures).

Reviews: They are limited to 20 pages in addition to supplementary materials (schemes, tables, figures, etc.).

- The original manuscript must be arranged as follows: Title page (including the title, authors and correspondence address), abstract, key words, introduction, materials and methods, results and discussion, acknowledgements and references.
- The reviews must be arranged as follows: Title page (including the title, authors and correspondence address), abstract, introduction, discussion, acknowledgements and references.

EMU Journal of Pharmaceutical Sciences
EMUJPharmSci

1. General Format

a) All manuscripts can only be submitted electronically via DergiPark.
b) Manuscripts should be 1,5 lines spaced and justified.
c) Use 2.5 cm margins, Times New Roman and format for A4 paper.
d) Number all pages, starting with the title page.
e) Spell out all acronyms in full at first use.
f) Make sub-headings if necessary.
g) Follow internationally accepted rules and conventions: use the international system of units (SI).

2. Before main text

A. Title page

a) The first page of the manuscript is a title page containing the following information:
b) The manuscript's full title (*Font: Times New Roman Font Size: 13*). The title must be concise and informative.
c) All authors' full names (*Font: Times New Roman Font Size: 11)*.
d) The affiliation of the author(s) should be linked by superscript numbers, and listed beneath the title.
e) Corresponding author (*Font: Times New Roman Font Size: 10)*. E-mail, telephone and fax number (with country and area code) of the corresponding author should be provided.
f) Ethical approval should be attached for manuscripts involving studies with human/laboratory animals participants.

B. Abstract

a) The abstract appears on its own page.
b) The abstract should be written in Times New Roman and font size 11.
c) The maximum length of the abstract is 200 words.
d) The abstract should contain the objectives, methods, results and conclusions.
e) 3- 6 key words must be provided in alphabetical order (Font: Times New Roman Font Size: 10). Separate the keywords with colon.

3. Main text

A. Introduction

(Font: Times New Roman Font Size: 12)
State the objectives of the work and provide a brief background of the literature related with the topic. The novelty and the aim of the study should be clearly stated.

B. Materials and Methods

(Font: Times New Roman Font Size: 12)

a) Give a brief and clear description of the materials and methods used. Subtitles can be given as appropriate.
b) For plant materials, herbarium name (or acronym), number, name and surname of the person who identified the plant materials should be indicated in this part of the manuscript.
c) Statistical analysis must be provided when necessary.

EMU Journal of Pharmaceutical Sciences
EMUJPharmSci

C. Results / Discussion

(Font: Times New Roman Font Size: 12)

A combined Results and Discussion section is often appropriate. Results should be concise.

Discussion should explore the significance of the results of the work.

Discussion should not repeat the results.

The main conclusions of the study should be presented.

D. Acknowledgement

(Font: Times New Roman Font Size: 10)

Supporting institutions or individuals should be briefly acknowledged just before the reference list.

E. References

i. Citation in text

(Font: Times New Roman Font Size: 12)

- Please ensure that every reference cited in the text is also present in the reference list (and vice versa).
- Unpublished results and personal communications are not recommended in the reference list.
- References in the text should be cited as: the author(s) surname and the publication date**.**

Examples:

(Sahin, 2000) – one author

(Sahin and Kosar, 2000) – Two authors

(Sahin *et al.,* 2000) – more than two authors

(Celik and Ozhatay 2000 a, b) – More than one paper in the same year by the same author (s)

(Ozhatay and Avci, 2000; Ozhatay *et al.,* 2001; Ozhatay, 2005) – listed by the earliest year first for multiple citations.

ii. Reference style

(Font: Times New Roman Font Size: 10)

- The list of references should be single-spaced.
- List the references in alphabetical order under section of "references".
- For references up to 5 authors, write the names of all authors.
- For references more than 5 authors, write the names of the first 5 and add *et. al.*
- The title of journal should be abbreviated in italics according to the style used in the National Library of Medicine's Journals in NCBI Databases.
- Volume numbers should be indicated in bold letters.

iii. Examples

Reference to a journal publication:

Ozhatay N, Kultur S, Gurdal B (2017). Check-list of additional taxa to the supplement flora of Turkey VIII. *Istanbul J Pharm* **47**(1): 31-46.

Reference to a book:

Strunk W Jr, White EB (1979). The Elements of Style. 3rd ed. New York, NY: Macmillan.

Reference to a chapter in an edited book:

Bonati A (1988). Industry and conservation of medicinal plants. In Akerele O, Heywood V, Synge H (eds). The Conservation Medicinal Plants p.141-148 Cambridge University Press UK.

Electronic resources:

World Nuclear Association (WNA) (2014). Radioisotopes in Medicine, http://www.world-nuclear.org/info/ Accessed 13.10.2014.

EMU
Journal of
Pharmaceutical
Sciences
EMUJPharmSci

4. After main text

Figures / Tables captions

- Use figures and tables when information cannot easily be stated or summarized in the manuscript itself.
- All the figures and tables must be referred to in the main body of the text.
- Tables and Figures should be numbered consequently in the order of appearance within the text, referred as “Table 1” and “Figure 1”.
- Descriptive titles should be given at the top of the tables and at the bottom of the figures.
- Figures should be prepared with the highest resolution and should be provided as a separate page following references.

Submission checklist

Check the following submission list before submit your manuscript:

- Full E-mail address, full postal address, telephone and fax number of the corresponding author.
- All necessary files have been uploaded.
- References are in the correct format for this journal.
- All references mentioned in the Reference list are cited in the text.
- All figure captions.
- All tables (including title, description, footnotes).
- For any further information please e-mail:
  emuj.pharmsci@emu.edu.tr

EMU Journal of Pharmaceutical Sciences
EMUJPharmSci

CONTENTS

Research articles

Review

Research Article EMUJPharmSci ISSN 2651-3587 https://dergipark.org.tr/emujpharmsci

EMU Journal of Pharmaceutical Sciences

EMUJPharmSci

Separation/preconcentration of antimony(III) by nickel/nickel boride nanoparticles prior to hydride generation atomic absorption spectrometric determination

Miray Kavas[1], Nur Aksuner[1,2], Raif Ilktac*[2], Emur Henden[1]

[1]University of Ege, Faculty of Science, Department of Chemistry, Izmir, Turkey.

[2]University of Ege, Central Research Testing and Analysis Laboratory Research and Application Center, Izmir, Turkey.

Abstract

A new, simple, fast and inexpensive method has been developed for the preconcentration of trace amounts of antimony(III) ions using nickel/nickel boride nanoparticles prior to their determination by hydride generation atomic absorption spectrometry. Optimization of the analytical parameters including initial pH, sorbent amount, contact time, sample volume, eluent type, and interference effects have been performed. Under the optimized conditions, the enrichment factor was 25 and the limit of detection was 0.02 µg/L. Calibration graph was obtained in the range of 0.08-0.80 µg/L with a correlation coefficient of 0.9924. The sorption capacity of the nickel/nickel boride nanoparticles was found to be as high as 2500 mg/g. The proposed method was applied to tap water and bottled drinking water. The quantitative recovery values were obtained in the range of 95-104 %. Langmuir and Freundlich adsorption models were evaluated and the results showed that the sorption process fitted the Langmuir isotherm and monolayer adsorption process occurred. The proposed method was validated with a certified reference material. With the high capacity of the novel nickel/nickel boride nanosorbent, dynamic calibration range with suitable limit of detection and quantification, suitable enrichment factor, rapidity and cost-effectiveness, the proposed method is ideal for the preconcentration and determination of antimony(III).

Keywords

Antimony, hydride generation atomic absorption spectrometry, nickel/nickel boride nanoparticles, preconcentration.

Article History

Submitted: 11 December 2019 Accepted: 04 March 2020 Published Online: March 2020

Article Info

***Corresponding author:** Raif Ilktac, **e-mail:** raifilktac@gmail.com

Research Article:
Volume: 3 Issue: 1 March 2020 Pages: 1-15

INTRODUCTION

Antimony exists in the environment due to human facilities and natural sources. Soil run-off and rock weathering are the main natural sources, whereas the traffic is the primary source of the human activitiessince numerous antimony-containing addditivesare used in car brake lines, flame retardants and tire vulcanization processes (Filella *et al*., 2002; Benzce*et al*., 1994; Berman, 1980). Antimony is potentially toxic at very low concentrations and inhalation of antimony compounds may lead to pneumonitis, fibrosis and bone marrow disease (Fowler and Goering, 1991). Antimony and its compounds are included in the priority pollutant list of Environmental Protection Agency of the United States (USEPA) and European Union (USEPA, 1976; Council of European Communities, 1976). The USEPA drinking water standards for maximum contaminant level goal (MCLG) and maximum contaminant level (MCL) for antimony are both stated as 6 µg/L (USEPA, 2003). The European Union established the maximum admissible concentration of antimony in drinking water as 5 µg/L (Council of European Communities, 1998).

Due to its toxicity, the development of sensitive and selective methods for the determination of trace levels of antimony in various samples is very important. The commonly used analytical methods for the determination of antimony include flame atomic absorption spectrometry (FAAS) (Titretir *et al*., 2012), electrothermal atomic absorption spectrometry (ET-AAS) (López-García *et al*., 2017; Rojas *et al*., 2007), inductively coupled plasma emission spectrometry (ICP-OES) (Ilander and Vaisanen, 2011; Biata *et al*., 2017), inductively coupled plasma-mass spectrometry (ICP-MS) (Lin *et al*., 2017), spectrophotometry (Frizzarin *et al*., 2016) and voltammetry (Renedo and Martinez, 2007). Hydride generation technique combined with atomic absorption spectrometry (HGAAS) is a simple and well established technique for the determination of antimony (Dedina and Tsalev, 1995). It is often difficult to determine the extremely low concentrations of antimony directly by most of the analytical techniques due their insufficient sensitivity or interference effects. Thus, preconcentration and separation of trace levels of antimony prior to the determination step are usually necessary. Various kinds of separation and preconcentration methods such as co-precipitation (Zhang *et al.,* 2007), liquid–liquid extraction (Fan, 2007; Li *et al*., 2008), high-performance liquid

chromatography (Fontanella *et al*., 2016; Müller *et al*., 2009) and solid-phase extractionhave been proposed (Yu *et al*., 2002; Erdem *et al*., 2005; Pacheco *et al*., 2007; Zih-Perenyi *et al*., 2008; Souza and Tarley, 2008). Different types of sorbents have been successfully used for the preconcentration of antimony(III) (Zheng *et al*., 2006; Nomngongo *et al*., 2013; Huang *et al*., 2007).

Design of novel nanomaterials has become of great importance since the last decade, due to awide range of applications that they have. Their novel optical, electronic, magnetic, and chemical properties that are ascribed to the extremely small dimensions and special surface nature have attracted the interest of analytical chemists on metallic nanoparticles (Starowicz *et al*., 2006; Welch and Compton, 2006; Lu *et al*., 2000). Nickel nanoparticles have important applications in catalytic reactions (Yoon *et al*., 2005). According to our knowledge, nickel containing nanoparticles have not been used for the preconcentration of antimony so far.

According to our previous observation on the determination of arsenic and antimony by HGAAS, the signal suppression of nickel(II) is due to the sorption of arsenic(III), arsenic(V) and antimony(III) ions by the black nickel/nickel boride nanoparticles generated via the reduction of sodium tetrahydroborate(III) (Henden *et al*., 2011). Therefore, in the present study, a novel procedure for the preconcentration and determination of antimony(III) at low concentration by HGAAS using nickel/nickel boride nanoparticles as sorbent has been proposed. For this purpose, nickel/nickel boride nanoparticles were prepared by the reduction of nickel(II) with sodium tetrahydroborate(III). The synthesized nanoparticles were utilized for the selective and sensitive preconcentration and determination of antimony. In order to determine the accuracy of the proposed method, certified reference material (CRM) was analysed and satisfactory results were obtained. The proposed method was also applied toreal water samples for the determination of trace antimony and quantitative recovery values were obtained. Because of the high capacity of the novel nickel/nickel boride nanosorbent, dynamic calibration range with suitable limit of detection (LOD) and limit of quantification (LOQ), rapidity and cost-effectiveness, the proposed method is thought to be an ideal method for the preconcentration and determination of antimony.

MATERIALS AND METHODS

Reagents

1000 mg/L stock solutions of antimony(III) were prepared by dissolving potassium antimony tartrate (Merck) in 2 M hydrochloric acid (HCl) (Merck). Lower concentration standards were prepared daily from the stock standards.

$NaBH_4$ solutions were prepared daily by dissolving sodium tetrahydroborate(III) pellets (Merck) in 0.15 M and 0.01 M NaOH, respectively. HCl and nitric acid (HNO_3) were purchased from Merck. 25 % Ni(II) solution was prepared by dissolving $Ni(NO_3)_2.6H_2O$ (Merck) in water and adjusting the final acidity to 0.004 M with HCl.

Apparatus

GBC 904 PBT model atomic absorption spectrometer (Illinois, USA) equipped with GBC HG3000 continuous-flow hydride generation system was used for antimony determination. Antimony hollow cathode lamp was operated with a maximum current of 10 mA at 217.6 nm and Deuterium (D_2) background correction was performed in all measurements. Air-acetylene flame was used for heating the quartz tube externally. Nüve water bath shaker (Ankara, Turkey) equipped with a thermostat was used for sorption studies. pH measurements were performed by using an Orion 4 Star pH meter (Beverly, USA). pH meter was calibrated before every measurement. For centrifugation, Nüve NF 800 (Ankara, Turkey) was used at 3000 rpm. All weight measurements were performed by using a Precisa XB220A balance (Dietikon, Switzerland). The morphologies of the nanoparticles were analyzed by scanning electron microscopy (SEM) (Thermo Fisher Scientific, Oregon, USA). X-ray photoelectron spectra (XPS) were recorded on a ThermoScientific K-alpha X-ray photoelectron spectrometer (Thermo Fisher Scientific, UK). Kα radiation was employed as the excitation source.

Procedure for the determination of antimony(III)

Unadsorbed antimony(III) remained in the solution was determined by using continuous flow HGAAS. In this system, sample, sodium tetrahydroborate(III) and acid solutions were introduced to the spectrometer with the aid of peristaltic pump after passing through the reaction loop and gas/liquid separator, respectively. Operating and working conditions of the system used for the determination of antimony are shown in Table 1.

Table 1: Instrumental operating parameters for the continuous-flow HGAAS in antimony determination.

Parameters	Continuous flow HGAAS
System type	Flame
Lamp current (mA)	10.0
Wavelength (nm)	217.6
Slit width	0.2
Sampling mode	Automated sampling
Flame type	Air-Acetylene
Acetylene flow rate (L/min)	2.10
Air flow rate (L/min)	13.50
Read time (s)	30
Measurement mode	Peak Area
Carrier gas	Nitrogen
N_2 flow rate (mL/min)	50
HCl (mol/L)	2.0
$NaBH_4$ (%)	0.6
HCl flow rate (mL/min)	2.0
$NaBH_4$ flow rate (mL/min)	2.0
Sample flow rate (mL/min)	8.0

Synthesis of nickel/nickel boride nanoparticles

Two mL 4 % $NaBH_4$ was added onto 10 mL of 1 g/L Ni(II) in 0.004 M HCl in a 50 mL beaker while stirring the solution with a magnetic stirrer. Black particles were formed immediately in the beaker and the particles were separated by centrifugation. The particles were washed with distilled water at least three times. The nanoparticles prepared with this procedure are called as oxic particles.

Preparation of the black nanoparticles was also performed under nitrogen atmosphere with the similar way. The nanoparticles prepared with this procedure are called as non-oxic particles.

Sorption and isotherm models

The sorption capacity and the percentage of antimony sorption were calculated respectively by the following equations:

$$Q = \frac{(C_i - C_e) \times V}{W} \qquad (3)$$

and

$$Sorption\ (\%) = \frac{(C_i - C_e)}{C_e} \times 100 \qquad (4)$$

Where Q represents the adsorption capacity (mg/g), C_i and C_e are the initial and equilibrium concentrations of antimony(III) ions (mg/L), respectively. W is the mass of sorbent (g) and V is the volume of the solution (L).

Freundlich and Langmuir models are the simplest and the most commonly used isotherms to simulate adsorption of components from a liquid phase onto a solid phase. The Langmuir model is a valid monolayer sorption on a surface containing a finite number of binding sites. It assumes uniform energies of sorption on the surface and no transmigration sorbate in the plane of the surface. The Freundlich equation is an empirical adsorption model. Langmuir and Freundlich isotherm models were applied by using the equations:

$$\frac{C_e}{C_s} = \frac{1}{Q_m L} + \frac{C_e}{Q_m} \quad (5)$$

and

$$\ln C_s = lnK_f + n_f lnC_e \quad (6)$$

where Q_m (mg/g) and L (L/mg) are Langmuir constants, Q_m is the amount of antimony ion sorption corresponding to monolayer coverage, L is the affinity of antimony for the sorbent, C_e (mg/L) is the amount of antimony in liquid phase at equilibrium and C_s (mg/g) is the amount of antimony adsorbed on the surface of the sorbent at equilibrium. K_f (mg/g) and n_f are the Freundlich constants (Limousin *et al*., 2007; Umpleby *et al*., 2001).

RESULTS AND DISCUSSION

Choise of sorbent for sorption of antimony(III)

In this study, sorption efficiencies of both oxic and non-oxic nickel/nickel boride nanoparticles were investigated for the sorption of antimony(III). 25 mL of 1000 µg/L antimony(III) solution at pH 6.0 was added onto 10 mg nickel/nickel boride nanosorbent and the mixture was shaken for 30 minutes at 25 °C. After sorption, the sorbent and the supernatant solution were separated by centrifugation. Then, the unadsorbed antimony(III) remained in the supernatant was determined by using continuous flow HGAAS. For the determination of the sorbed antimony, the sorbent was dissolved in 3 mL of concentrated HCl and the procedure explained above was applied for the determination of sorbed antimony. The sorption efficiencies of oxic and non-oxic nickel/nickel boride nanoparticles were found to be 99.2±1.7 % and 100.0±1.8 % (n=5), respectively. Since the sorption efficiencies were quantitative and comparable, non-oxic nickel/nickel boride nanoparticles were chosen to be used as sorbent for the determination and preconcentration of antimony(III).

Characterization of the sorbent

Characterization of the non-oxic nickel/nickel boride nanoparticles was performed by using SEM and XPS. The morphologies of the synthesized nanoparticles are shown in SEM images in Figure 1. According to the XPS results, the structure of the sorbent was suggested to be the mixture of Ni_xB, Ni(0) and $Ni(OH)_2$ (Figure 2) (Henden *et al*., 2011).

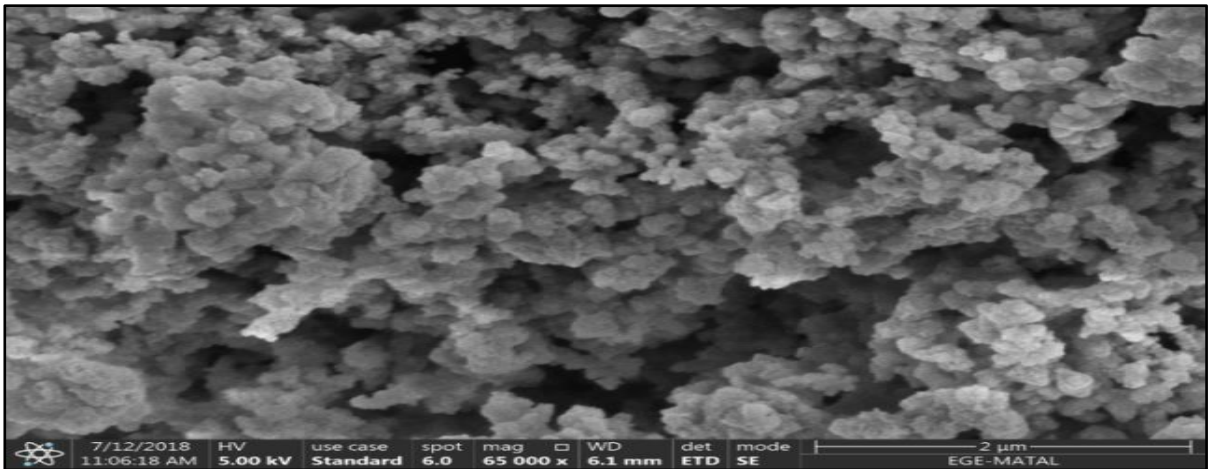

Figure 1: SEM image of nickel based nanoparticles.

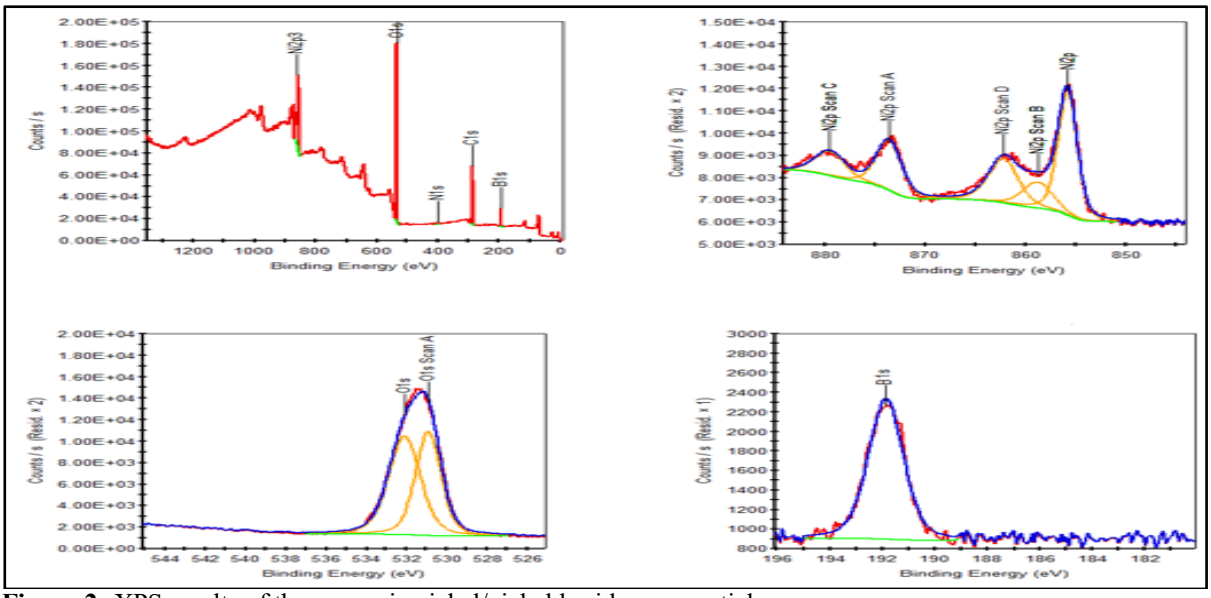

Figure 2: XPS results of the non-oxic nickel/nickel boride nanoparticles.

Effect of pH

pH values of antimony(III) solutions were adjusted using dilute HCl or sodium hydroxide solutions. The effect of initial pH on the sorption of antimony(III) was investigated within the range of 3-10. 25 mL 1000 µg/L antimony(III) solutions with different pH values were added onto 10 mg sorbent. After centrifugation, unadsorbed antimony was determined. As shown in Figure 3, the quantitative sorption efficiencies for antimony(III) were obtained in the range of pH 3-10. The pH did not have a significant effect on the sorption efficiency and the initial pH of the solutions was adjusted to pH 6.0 for the further analyses.

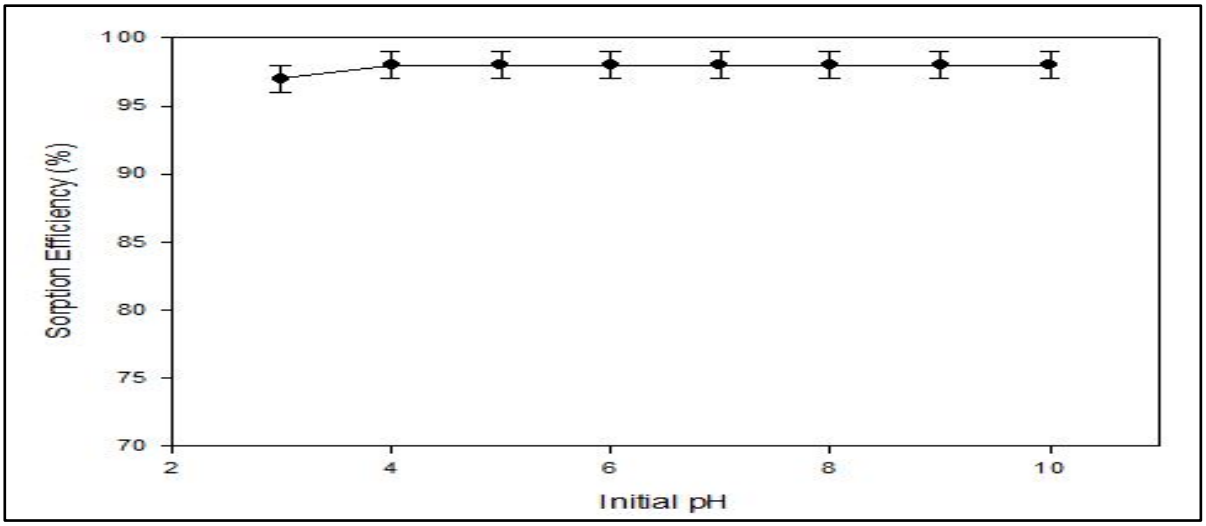

Figure 3: The effect of initial pH on antimony sorption efficiency (Sorbent amount: 10 mg, 25 mL 1000 µg/L antimony(III) solution).

Effect of the sorbent amount

In order to determine the effect of the amount of the sorbent on the preconcentration of antimony, 25 mL of 1000 µg/L antimony(III) solution was shaken with different amounts (10 to 60 mg) of non-oxic nickel/nickel boride nanoparticles and unadsorbed antimony(III) remained in the solution was measured.

Quantitative recoveries (>96 %) of antimony(III) were attained in all of the dosages used. Therefore, further studies were performed with 10 mg of the sorbent.

Effect of contact time

In order to determine the optimumcontact time on antimony sorption efficiency, 25 mL of 1000 µg/L antimony(III) solutions at pH 6.0 were shaken with 10 mg of the sorbent with different contact times (10-120 minutes) at 25 ºC. After centrifugation, the unadsorbed antimony(III) concentration in solution was determined. As shown in Figure 4, optimum contact time for antimony sorption was chosen as 30 minutes that was used in the futher analyses.

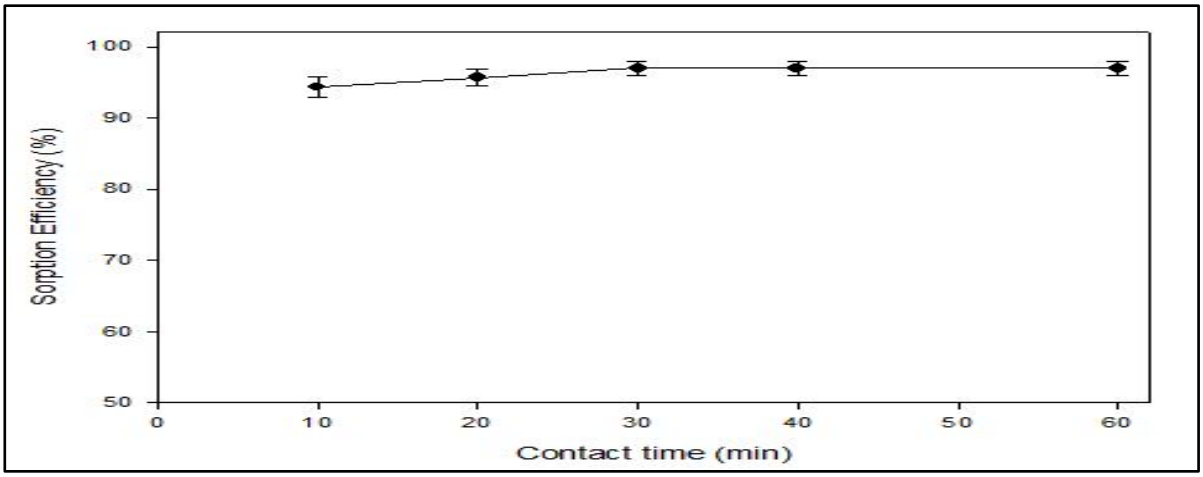

Figure 4: The effect of contact time on antimony sorption (Sorbent amount: 10 mg, 25 mL 1000 µg/L antimony(III) solution at pH 6.0).

Effect of sample volume

The effect of the sample solution volume on the antimony(III) sorption was investigated by shaking 25-250 mL of 1000 µg/L antimony(III) solution (pH 6.0) with 10 mg sorbent for 30 minutes at 25°C. After sorption, the unadsorbed antimony was determined. As shown in Figure 5, the sorption of the antimony(III) was quantitative and was not affected by the volume of the sample up to 250 mL.

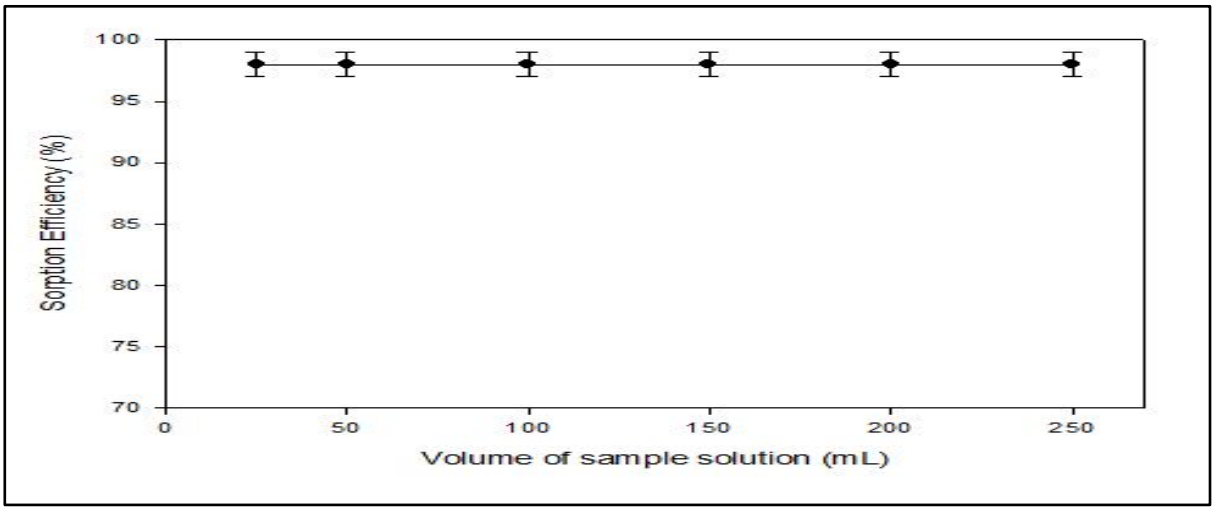

Figure 5: Effect of sample solution volume on the sorption efficiency (Sorbent amount: 10 mg, 1000 µg/L antimony(III) solution at pH 6.0).

Antimony recovery

Different concentrations of HCl, nitric acid, sulfamic acid and ascorbic acid were used to recover the adsorbed antimony. However, antimony(III) could not be desorbed quantitatively without decomposing the sorbent. Among the reagents used, concentratedhydrochloric acidprovided the highest recovery (99.3±1.2, n=3) and therefore concentrated hydrochloric acid was selected as recovery

agent in the further studies. In recovery studies, to eliminate the nickel(II) interference on antimony(III) detection, 0.01 M EDTA was added to the solution.

Sorbent Capacity

In order to determine the sorption capacity of the sorbent, 10 mg non-oxic nickel/nickel boride nanoparticles wereshaken with 50 mL of 500 mg/L antimony(III) solution (pH ~6.0). After shaking for 30 minutes, the phases were separated by centrifugation, the sorbent was dissolved in 3 mL of concentrated HCl and the solution volume was adjusted to 25 mL. Then, antimony concentration in the solution was measured by continuous flow-HGAAS. The sorption capacity (Q, mg/g) was calculated by using the equation (3) and the results showed that the maximum amount of antimony(III) ions that can be adsorbed by the nickel/nickel boride nanoparticles was found to be 2500 mg/g. This value is unexpectedly high when compared to that in the literature (Table 2).

Table 2: Comparison of the proposed method with other reported methods for preconcentration of antimony(III).

Adsorbent	Linear range (µg/L)	Detection limit (µg/L)	Enrichment Factor	Adsorption capacity (mg/g)	Detection	Reference
Magnetic core-modified silver nanoparticles	0.05–2.5	0.03	325	10	ET-AAS	10
Isolute silica-based octyl (C8) sorbent	0–5.0	0.001	N.R.*	N.R.*	ICP-MS	23
–SH functional groups (Duolite GT-73)	0–80.0	0.06	N.R.*	N.R.*	HG-AAS	24
L-methionine	0.07–100	0.07	20	N.R.*	ICP-OES	25
Imino diacetic acid–ethyl cellulose	1–4	0.18	25	N.R.*	ET-AAS	26
Ammonium O,O- diethyl dithiophosphate	0.25-16	0.08	229	N.R.*	GF-AAS	27
Nanometer size titanium dioxide (rutile)	N.R.*	0.05	50	>29.6	HG-AAS	28
SPE-Dowex 1-x8	N.R.*	0.05	4	N.R.*	ICP-OES	29
Akaganeite	N.R.*	N.R.*	N.R.*	61.2	ICP-MS	38
Nano titania-chitosan beads	N.R.*	N.R.*	N.R.*	60.03	ICP-OES	39
Nickel/nickel boride nanoparticles	0.08–0.80	0.02	10	2500	HG-AAS	This study

*Not Reported.

Adsorption isotherms

The adsorption isotherm of the sorption of antimony(III) onto nickel/nickel boride nanoparticles was determined. In order to identify the adsorption type and determine the adsorption capacity, 10 mg non-oxic nickel/nickel boride nanoparticles were added to 10 mL of antimony(III) solution (20–3000 mg/L, pH~6) and the mixture was shaken for two hours at room temperature to reach the equilibrium. Then, unadsorbed antimony(III) concentration in the solution was measured by continuous

flow-HGAAS. By using equations (5) and (6), the correlation coefficient (R^2) for Freundlich isotherm and Langmuir isotherm was found to be 0.7442 and 0.9986, respectively. Thus, it can be concluded that the adsorption processfitted to Langmuir isotherm and monolayer adsorption process occurred. Sorption capacity of the sorbent was found to be 2500 mg/g from the Langmuir equation andwasin accordance with the experimental value obtained from equation (3).

Analytical performance

Under the optimal conditions of the preconcentration, linear calibration graph was obtained within the concentration range of 0.08-0.80 µg/L by 25 times preconcentration. The calibration equation was $A=0.4238C_{Sb} + 0.1887$ ($R^2 = 0.9924$), where A is absorbance, and C_{Sb} is the concentration of antimony(III) in µg/L. The limit of detection (LOD) and the limit of quantification (LOQ) can bedefined as;

$$LOD = \frac{\sigma}{S} \times 3 \qquad (1)$$

and

$$LOQ = \frac{\sigma}{S} \times 10 \qquad (2)$$

where σ is the standard deviation of the responses of blank solution and S is the slope of the calibration curve. LOD and LOQ were found to be 0.020 µg/L and 0.066 µg/L, respectively. Precision of the proposed method was determined as 1.9 % for six replicated determination of 0.12 µg/L of antimony(III) for 50 mL solution.

The proposed method was compared toother preconcentration procedures that are currently used for the determination of antimony and the results are summarized in the Table 2. LOD of the method was comparable to that obtained by other estalished methods and the capacity of the sorbent was much higher than other reported sorbents. Therefore, it was concluded that the proposed method is suitable for the preconcentration and determination of trace levels of antimony(III) and the novel sorbent with ultra-high-capacity is also suitable for antimony(III) removal.

Interferences study

In order to identify the potential interferences in the preconcentration of antimony using the proposed sorbent, the effects of some diverse ions, which may be present in real samples, were evaluated. In order to evaluate the interference effect, various excess amounts of diverse ions were added onto 25 mL of 50.0 µg/L of antimony(III) (pH~6) and the proposed procedure for determination of adsorbed antimony(III) was applied. An ion was considered as an interfering agent when its presence produced more than ±5.0 % change in the antimony signal. The results are summarized in Table 3. The results showed that excess amounts of common

cations do not interfere the determination of trace quantities of antimony(III). Therefore, the proposed preconcentration procedure described not only preconcentrated the antimony but also eliminated such interferences.

Table 3: Tolerable concentration ratio of diverse ions to antimony(III).

Co-existing diverse ions	Diverse ion to analyte concentration ratio
copper(II), zinc(II), cobalt(II), nickel(II)	1000
iron(III), cadmium(II), aluminium(III)	500
tin(II), lead(II)	200
arsenic(III)	50

Accuracy of the method

For the evaluation of the accuracy of the proposed method, certified reference material (drinking water-LOW, EnviroMAT, EP-L-2) was analyzed for antimonyin three replicates after preconcentration procedure. The measured value (0.011 ± 0.004 mg/L) was in good agreement with the certified value (0.012 ± 0.005 mg/L).

Analytical application

The proposed method was applied to tap water, commercially bottled drinking water and mineral water to determine the amount ofantimony(III). The pH of the sample was adjusted to ~6.0 and shaken with 10 mg sorbent for two hours.

After sorption, the phases were separated and adsorbed antimony(III) was measured. Antimony(III) was not detected in any of the water samples and therefore, spike addition method was applied. The results shown in Table 4 indicated that the recoveries were quantitative for trace antimony analysis, ranging from 95 to 104 %.

As a conclusion, in the present study, nickel/nickel boride nanoparticles was successfully synthesized and used for the preconcentration and determination of antimony(III) by HGAAS. The proposed method was compared to the other preconcentration procedures that are currently used for the determination of antimony. LOD of the method was comparable to that obtained by other estalished methods. The sorption capacity was much higher than the other sorbents reported. Therefore, the sorbent was suggested for antimony removal. Furthermore, the preparation of the sorbent is simple and cost effective. The established preconcentration procedure is simple, rapid, economic and reliable. The method was validated with the analysis of a certified reference material. The proposed method was applied for the determination of antimony(III) in water samples and satisfactory results were obtained. The proposed preconcentration procedure was also shown to be successful

for eliminating serious interferences of several ions at high concentration improving the applicability of hydride generation based atomic spectrometric techniques.

Table 4: Results of the determination of antimony(III) in different water samples.

Sample	Added (µg/L)	Found[a] (µg/L)	Recovery (%)
Tap water	-	BLD[b]	-
	10	10.3 ± 0.2	103.0±2.0
	20	19.4 ± 0.3	97.2±1.8
Drinking water 1	-	BLD[b]	-
	10	9.6 ± 0.1	96.0±1.0
	20	20.3 ± 0.4	101.6±1.9
Drinking water 2	-	BLD[b]	-
	10	9.8 ± 0.5	98.0±5.0
	20	19.0 ± 0.4	95.2±2.5
Mineral water 1	-	BLD[b]	-
	10	10.4 ± 0.6	104.0±6.0
	20	20.2 ± 0.3	101.0±2.6
Mineral water 2	-	BLD[b]	-
	10	9.5 ± 0.5	95.0±5.0
	20	20.4 ± 0.4	102.0±4.0

[a] Mean ± standard deviation, n=3.
[b] BLD= Below the limit of detection.

ACKNOWLEDGEMENTS

The study was financially supported by the Ege University Research Fund, Project No: 2009 FEN 078.

REFERENCES

Bencze K, Seiler HG, Sigel A, Sigel H (Eds.) (1994). Handbook on Metals in Clinical and Analytical Chemistry, Marcel Dekker, New York, 223-228.

Berman E (1980). Toxic Metals and their Analysis. Heyden, London.

Biata NR, Nyaba L, RamontjaJ, Mketo N, Nomngongo PN (2017). Determination of antimony and tin in beverages using inductively coupled plasma-optical emission spectrometry after ultrasound-assisted ionic liquid dispersive liquid-liquid phase microextraction *Food Chem.* **237**: 904–911.

Council of the European Communities (1976). L129, 23.

Council of the European Communities (1998). Council directive relating to the quality of water intended for human consumption (98/83/CE).

Dedina J, Tsalev DL (1995). Hydride generation atomic absorption spectrometry, Wiley, Chichester.

Erdem A, Eroglu AE (2005). Speciation and preconcentration of inorganic antimony in waters by Duolite GT-73 microcolumn and determination by segmented flow injection-hydride generation atomic absorption spectrometry (SFI-HGAAS). *Talanta.* **68**: 86-92.

Fan Z (2007). Determination of antimony(III) and total antimony by single-drop microextraction combined with electrothermal atomic absorption spectrometry. *Anal Chim Acta.* **585**: 300-304.

Filella M, Belzile N, Chen YW (2002). Antimony in the environment. A review focused on baturals waters. *Earth Sci Rev.* **57**: 125–176.

Fontanella MC, Beone GM, Cattani I (2016). Determination of Sb(III) and Sb(V) by HPLC-Online isotopic dilution- ICP MS. *MethodsX*. **3**: 102–109.

Frizzarin RM, Portugal LA, Estela JM, Rocha FR, Cerdà V (2016). On-line lab-in-syringe cloud point extraction for the spectrophotometric determination of antimony. *Talanta.* **148**: 694–699.

Fowler BA, Goering PL (1991). Antimony. In: Merian E, ed. Metals and their compounds in the environment: occurrence, analysis, and biological relevance.Weinheim, VCH, pp. 743-750.

Henden E, Islek Y, Kavas M, Aksuner N, Yayayuruk O, Ciftci TD, Ilktac R (2011). A study of mechanism of nickel interferences in hydride generation atomic absorption spectrometric determination of arsenic and antimony. *Spec Chim Acta B.* **66**: 793-798.

Huang C, Hu B, Jiang Z (2007). Simultaneous speciation of inorganic arsenic and antimony in natural waters by dimercaptosuccinic acid modified mesoporous titanium dioxide micro-column on-line separation and inductively coupled plasma optical emission spectrometry determination. *Spectrochim Acta B.* **62**: 454-460.

Ilander A, Vaisanen A (2011). The determination of antimony and arsenic concentrations in fly ash by hydride generation inductively coupled plasma optical emission spectrometry. *Anal Chim Acta.* **689**: 78-183.

Kolbe F, Weiss H, Morgenstern P,Wennrich R, Lorenz W, Schurk K, Stanjek H, Daus BJ (2011). Sorption of aqueous antimony and arsenic species onto akaganeite. *Colloid Interface Sci*. **357**: 460–465.

Limousin G, Gaudet JP, Charlet L, Szenknect S, Barthes V, Krimissa M (2007). Sorption Isotherms: A Review on physical bases, modeling and measurement. *Appl Geochem.* **22**: 249-275.

Lin YA, Jiang SJ, Sahayam AC (2017). Determination of antimony compounds in waters and juices using ion chromatography-inductively coupled plasma mass spectrometry. *Food Chem*. **230**: 76–81.

Li Y, Hu B, Xiang G (2008). Simultaneous speciation of inorganic selenium and antimony in water samples by electrothermal vaporization inductively coupled plasma mass spectrometry following selective cloud point extraction. *Water Res.* **42**: 1195-1203.

López-García I, Rengevicova S, Muñoz-Sandova lMJ, Hernández-Córdoba M (2017). Speciation of very low amounts of antimony in waters using magnetic core modified silver nanoparticles and electrothermal atomic absorption spectrometry. *Talanta.* **162**: 309–315.

Lu L, Wang LB, Ding BZ (2000). High-tensile ductility in nanocrystalline copper. *J Mater Res* **15**:270-273.

Müller K, Daus B,Mattusch J, Stärk HJ, Wennrich R (2009). Simultaneous determination of inorganic and organic antimony species by using anion exchange phases for HPLC–ICP-MS and their application to plant extracts of *Pteris vittata. Talanta.***78**: 820–826.

Nishad PA, Bhaskarapillai A, Velmurugan S (2017). Enhancing the antimony sorption properties of nano titania-chitosan beads using epichlorohydrin as the crosslinker. *J Hazard Mater.* **334**: 160–167.

Nomngongo PN, Ngila JC, Kamau JN, Msagati TAM, Moodley B (2013). Preconcentration of molybdenum, antimony and vanadium in gasolsine samples using Dowex 1-x8 resin and their determination with inductively coupled plasma–optical emission spectrometry. *Talanta*. **110**: 153–159.

Pacheco PH, Gil RA, Martinez LD, Polla G, Smichowski P (2007). A fully automated system for inorganic antimony preconcentration and speciation in urine. *Anal Chim Acta.* **603**: 1-7.

Renedo OD, Martinez MJA (2007). A novel method for the anodic stripping voltammetry determination of Sb(III) using silver nanoparticle-modified screen-printed electrodes. *Electrochem Commun.* **9**: 820-826.

Rojas FS, Ojeda CB, Pavon JMC (2007).Preconcentration of inorganic antimony(III) in environmental samples by PSTH-Dowex microcolumn and determination by FI-ETAAS. *Talanta.* **72**: 951-956.

Souza JMO, Tarley CRT (2008). Preconcentration and speciation of Sb(III) and Sb(V) in water samples and blood serum after cloud point extraction using chemometric tools for optimization. *Anal Lett.* **41**: 2465–2486.

Starowicz M, Stypuła B, Banas J (2006). Electrochemical synthesis of silver nanoparticles. *Electrochem Commun.* **8**: 227-230.

Titretir S, Sık AI, Arslan Y, Ataman OY (2012). Sensitivity improvement for antimony determination by using in-situ atom trapping in a slotted quartz tube and flame atomic absorption spectrometry. *Spectrochim Acta B*. **77**: 63–68.

United States Environmental Protection Agency (USEPA) (1979). Water Related Fate of the 129 Priority Pollutants, EP-440r4-79-029A.

USEPA National Primary Drinking Water Standards (2003). Office of Water (4606M), EPA 816-F-03–016.

Umpleby RJ, Baxter SC, Bode M, Berch Jr JK, Shah RN, Shimizu KD (2001).Characterization of molecularly imprinted polymers with the Langmuir−Freundlich isotherm. *Anal Chim Acta.* **435**: 35-42.

Welch CM, Compton RG (2006). The use of nanoparticles in electroanalysis: a review. *Anal Bioanal Chem.* **384**: 601-619.

Yoon M, Kim Y, Kim YM, Volkov V, Song HJ, Park YJ, Park IW (2005). Superparamagnetic properties of nickel nanoparticles in an ion-exchange polymer film. *Mater Chem Phys.* **91**: 104-107.

Yu C, Cai Q, Guo ZX, Yang Z, Khoo SB (2002). Antimony speciation by inductively coupled plasma mass spectrometry using solid phase extraction cartridges. *Analyst.* **127**: 1380-1385.

Zih-Perenyi K, Jankovics P, Sugar E, Lasztity A (2008). Solid phase chelating extraction and separation of inorganic antimony species in pharmaceutical and water samples for graphite furnace atomic absorption spectrometry. *Spectrochim Acta Part B.* **63**: 445-449.

Zhang L, Morita Y, Sakuragawa A, Isozaki A (2007). Inorganic speciation of As(III, V), Se(IV, VI) and Sb(III, V) in natural water with GF-AAS using solid phase extraction technology. *Talanta.* **72**: 723-729.

Zheng FY, Qian SH, Li SX, Huang XQ, Lin LX (2006). Speciation of antimony by preconcentration of Sb(III) and Sb(V) in water samples onto nanometer-size titanium dioxide and selective determination by flow injection–hydride generation– atomic absorption spectrometry. *Anal. Sci.***22**: 1319-1322.

Research Article EMUJPharmSci ISSN 2651-3587 https://dergipark.org.tr/emujpharmsci

EMU Journal of Pharmaceutical Sciences

EMUJPharmSci

Anatomical studies of *Dracocephalum moldavica* L., *Ocimum basilicum* L. and *Agastache rugose* (Fisch. & C.A.MEY) Kuntze (Lamiaceae) used for cardiovascular diseases in traditional Uyghur medicine

Nuerbiye Aobuliaikemu, Mine Kocyigit*

Istanbul University, Faculty of Pharmacy, Department of Pharmaceutical Botany, Istanbul, Turkey.

Abstract

Traditional Uyghur Medicine (TUM) is widely used in Xinjiang Uyghur Autonomous Region in the east-west of China. TUM divided cardiovascular diseases according to causes and symptoms into several different types with different treatments to gain effective results. In this study, it was attempted to research anatomical characteristics of three frequently used herbs in cardiovascular disease treatments in TUM: *Dracocephalum moldavica, Ocimum basilicum,* and *Agastache rugosa*, all from Lamiaceae family. Leaf and stem anatomies of these three plants were examined in detail.

Keywords

Agastache rugose, Dracocephalum moldavica, Ocimum basilicum, TUM.

Article History

Submitted: 17 December 2019 Accepted: 23 March 2020 Published Online: March 2020

Article Info

***Corresponding author:** Mine Kocyigit, **e-mail:** minekocyigit@hotmail.com

Research Article:

Volume: 3 Issue: 1 March 2020 Pages: 16-28

INTRODUCTION

The history of Traditional Uyghur medicine (TUM) can be traced back to 2500 years ago (Zhao *et al.,* 2017). TUM interacted with other medical theories, such as traditional Chinese Medicine, ancient Greece medicine, Egyptian Medicine, Arabian Medicine, and Indian Medicine throughout history. Currently, it has formulated a sophisticated and systematic theoretical system (Umar *et al.,* 2015). It is composed of different fundamental theories such as Erkan theory (fire, air, water, earth), four temperaments (cold, heat, moist, dry) and the four body fluids, also called Humor (blood, phlegm, yellow bile, black bile) (Mattohti, 2015; Aibai, 2007).

TUM divided cardiovascular diseases into two types: Humoral and non-humoral. Depending on the cause of the disease, TUM grouped them into cold, hot, dry and moisture-induced types. Treatments are applied according to the groupings, mentioned above, and the symptoms such as, heart palpitations, heart pain, heart pressure, heart 'chi' progression, angina, high blood pressure (Aibai, 2007). Mixed herbal preparations are preferred to be used instead of single herb usages and three Lamiaceae herbs, *Dracocephalum moldavica* L., *Ocimum basilicum* L., *Agastache rugosa* (Fisch. & C.A.Mey.) Kuntze are frequently chosen.

D. moldavica is an annual herb, which is distributed in China, Russia, Siberia, Eastern Europe, Central Europe and South to Kashmir (Flora of Xinjiangensis, 2004). The root or the whole plant of *D. moldavica* has medicinal value with clinical applications (Chinese Materia Medica, 2005). The main components of the aromatic oil (oil content is 0.01-0.17 %) obtained from the whole grass are citral (25-68 %), geraniol (80 %), nerol (7 %) and thymol (Feng and Li, 2015). It has extensive usage both in Uyghur Medicine and Tibet Medicine for cold, headache, sore throat, bronchitis, asthma, jaundice, vomiting, blood stasis, dysentery, heart disease, neurasthenia and also it is used as an anticancer agent (Miernisha *et al.,* 2015).

O. basilicum is an annual herb. The herb sweet basil is native to tropical Asia, Africa and America. It was being cultivated in Eygpt 300 years ago, reached England in 16th century, and North America in 17th century, and currently it is cultivated all over the world. The entire plant contains volatile oil and coumarins. Flowers contain ursolic acid, oleanolic acid, and β-sitosterol. Seeds contain oil over 16.8 % (Yi *et al.,* 2004). Moreover, it

is used for the treatment of cardiac insufficiency, heart fibrillation, cold cough and diarrhea in TUM (Umar *et al.,* 2014).

A. rugosa is commonly known as the Korean mint, and its native range is from Russian Far East to East Asia. Major components are essential oil (0.28 %) which mainly consists of more than 80 % is methylchavicol (Chinese Materia Medica, 2005). It is used as a supplement for spleen, stomach and liver disorders. Also, sometimes it is used as an anti-depressant (Gong *et al.,* 2017).

The present study aims to investigate the anatomical and morphological alterations taking place in the stem and leaves of three Lamiaceae plants that are used for cardiovascular diseases in TUM in order to assist in the identification of the plant materials.

MATERIALS AND METHODS

All samples were collected from Karakash, Xinjiang, China, in 2015. The voucher specimen was identified by the authors and deposited at the Herbarium of Faculty of Pharmacy, Istanbul University (ISTE). The Voucher numbers are ISTE 115639 for *D. moldavica,* NU 37 for *A. rugose,* ISTE 115640 for *O. basilicum.* Fresh stems and leaves were cut from specimens and put into a 70 % ethyl alcohol solution. Transverse and longitudinal sections of the samples were prepared freehand using razor blades. The sections were placed on glass slides and then stained with SARTUR solution (Celebioglu and Baytop, 1949). Several slides were made and photographed for each species with the aid of a light microscope (Olympus BH-2 and Canon A 640 digital camera).

RESULTS

D. moldavica L.

Stem anatomy

In transection, the stem presented a square shape. The epidermis appears in a single layer with thick, papillae cuticle. Intense glandular and non-glandular trichomes can be observed. The top of most of the non-glandular trichomes is multicellular. Most of the glandular trichomes were composed of a single row cell, the head of which are multiple, large-scale cells. The cortex is formed by 4-5 layers angular collenchyma cells with thickened at the corner and sclerenchyma among them. The vascular cylinder presents a thin phloem outward and thick xylem inward. The pith is

composed of broad parenchymatous cells with thin walls. Sclerenchyma is also located in the perimedullary region (Figure 1).

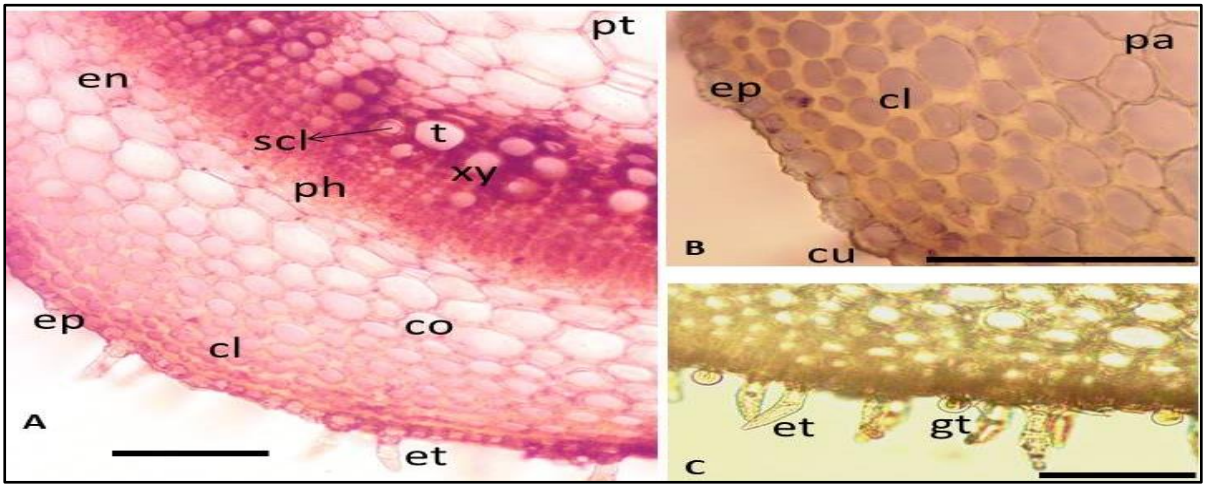

Figure 1: A) Stem anatomy of *D. moldavica,* B) Collenchyma, C) Trichomes:
ep: epidermis, gt: glandular trichome, cu: cuticle, pa: parenchyma, cl: collenchyma, et: eglandular trichome, en: endodermis, ph: phloem, xy: xylem, t: trachea, scl: sclerenchyma, pt: pith region, co: cortex (scale 0.1 mm).

Leaf anatomy

Cross-section of the bifacial blades reveals the upper epidermis, the mesophyll, and the lower epidermis. The upper and lower epidermis, one layer and isodiametric, were both composed of a row of thick radical walls and cuticles, and lower epidermis has thicker radical walls. They are amphistomatic leaves. The epidermal glandular and non-glandular trichomes and stomata are distributed on both epidermises. There are several types of glandular trichomes, one of which is the characteristic Lamiaceae family: single stalk cell and eight head cells. The non-glandular trichome observed in the leaf corresponds to the same type found in the stem (Figure 2). The leaf is dorsiventral and is formed by two layers of palisade and 4-5 layers of spongy parenchyma. The palisade parenchyma was composed of two layers of cells, which were smaller and more elongated at the inner layer. In some sectors, it was difficult to distinguish. The spongy parenchyma had 4-5 layers of cells with various shapes loosely arranged. Secondary vascular systems can be observed.

The leaf is amphistomatic. In both upper and lower epidermis, stomata are diacytic type with two subsidiary cells, and one is bigger than the other. The anticlinal walls are wavy. There are more glandular trichomes and non-glandular trichomes on the lower epidermis, and the non-glandular trichomes observed in the leaf corresponds to the same type found in the stem (Figure 3).

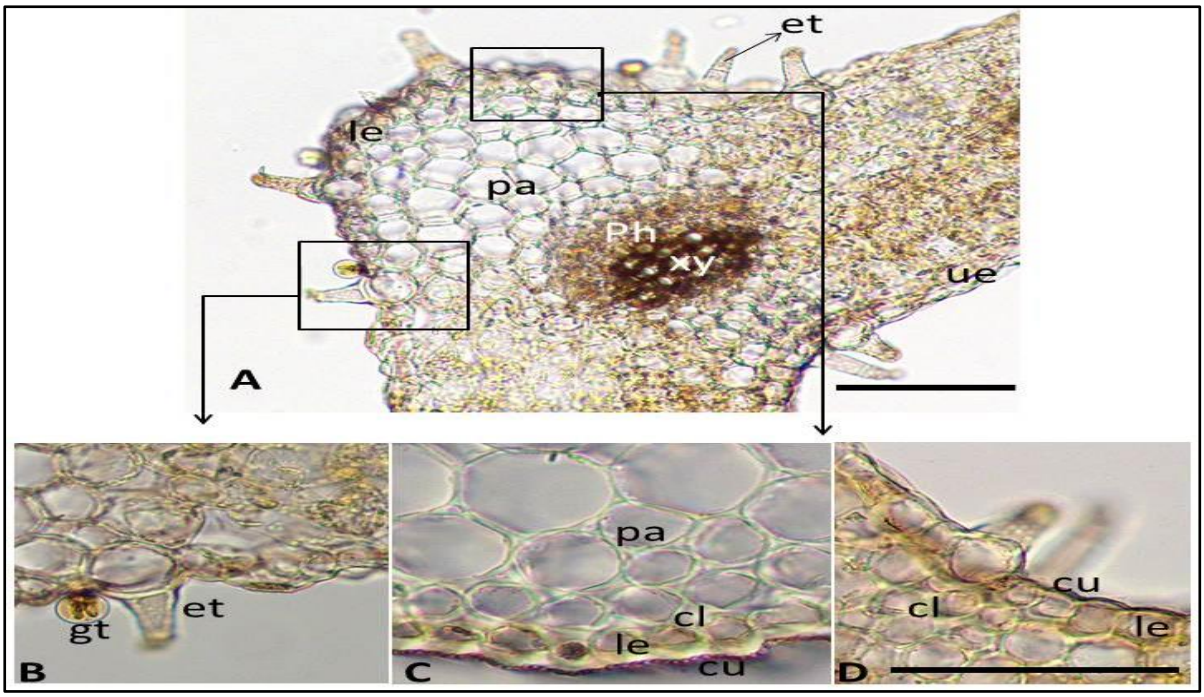

Figure 2: A) Midrib area in leaf of *D. moldavica,* B) Trichomes, C-D) Cuticle
ue: upper epidermis, le: lower epidermis; et: eglandular trichome, pa: parenchyma, ph: phloem, xy: xylem, gt: glandular, cu: cuticle, cl: collenchyma (scale 0.1 mm).

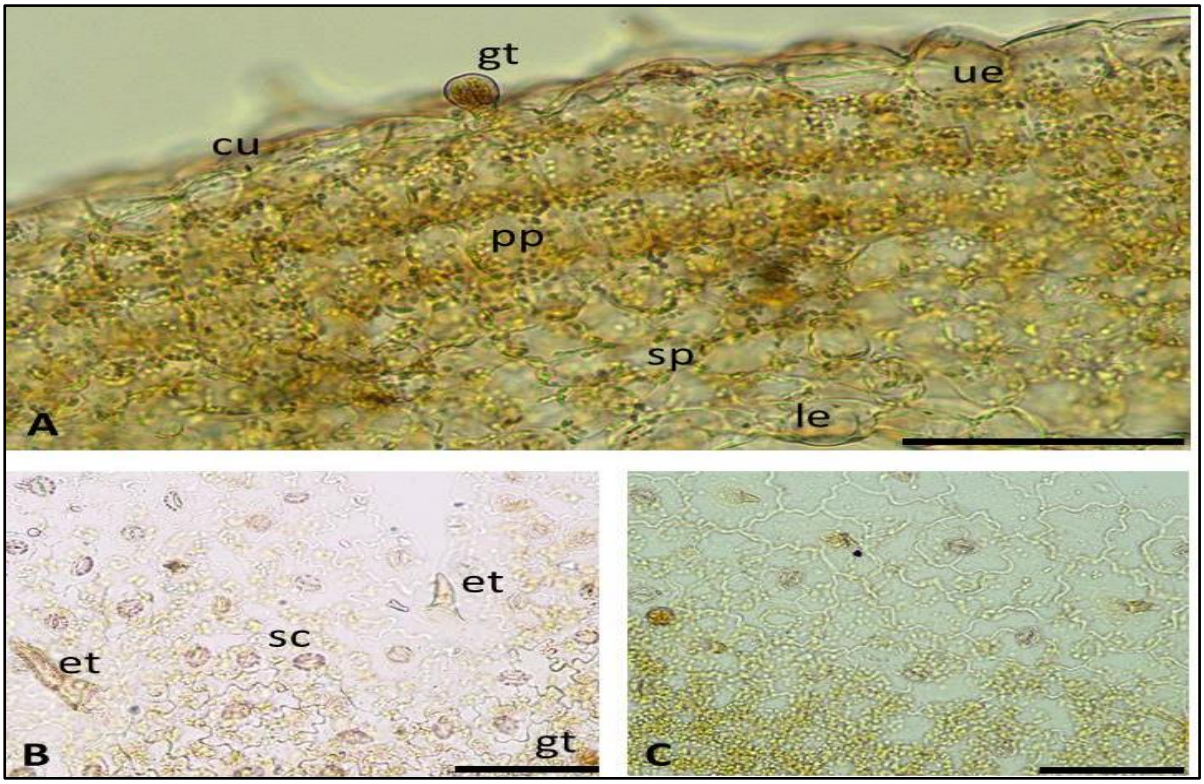

Figure 3: A) Leaf anatomy of *D. moldavica,* B) Upper epidermis, C) Lower epidermis.
ue: upper epidermis, gt: glandular trichome, le: lower epidermis, cu: cuticle, pp: palisade parenchyma, sp: spongy parenchyma, et: eglandular trichome, sc: stoma cell (scale 0.1 mm).

***O. basilicum* L.**

Stem anatomy

The overall appearance is rectangular, with a large pith area. It shows a typical character, consists of 3 parts; epidermis, cortex, central cylinder. Epidermis is a single-row, thickened outer wall with rectangular cells and is covered with cuticle and cuticle is flat. It is covered with glandular and non-glandular trichomes (Figure 4).

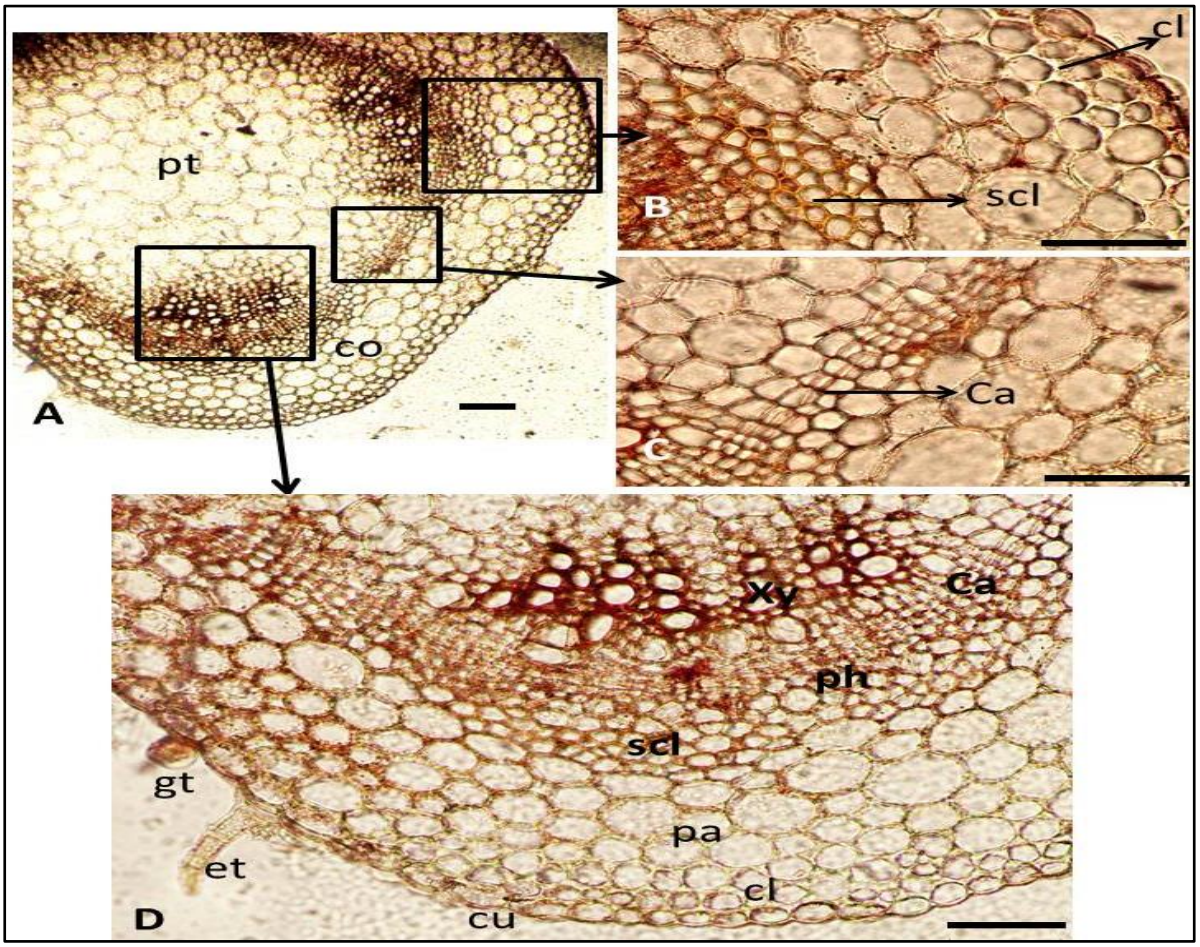

Figure 4: A) Stem anatomy of *O. basilicum*, B) Cortex, C) Cambium, D) Vascular tissues.
ep: epidermis, gt: glandular trichome, cu: cuticle, ca: cambium, pa: parenchyma, cl: collenchyma, et: eglandular trichome,en: endodermis, ph: phloem, xy: xylem, t: trachea, scl: sclerenchyma, pt: pith region, co: cortex (scale 0.1 mm).

Leaf anatomy

In the transverse section, the leaf is bifacial. The epidermis is uniseriate and covered by a thin cuticle with intense non-glandular trichomes, which has two or three bifurcated hooks and characteristic Lamiaceae family glandular trichomes. The collenchyma is a single layer. The collateral vascular system is surrounded by a thin uniseriate sclerenchyma cell (Figure 5).

In mesophyll, the upper epidermis is manifesting 1-2 rows of palisade parenchyma, then 3-4 rows of oval or round shaped sponge parenchyma with

irregular spaces between cells. The lower epidermis cells are smaller than the upper. Both epidermises are composed of ellipse-shaped cells without spaces among them. The epidermis on both sides are covered with a cuticle and some glandular and non-glandular hairs on them (Figure 6).

The leaf is amphistomatic. In both upper and lower epidermis, stomata are diacytictype with two subsidiary cells, and one is bigger than the other. The anticlinal walls are wavy. There are more glandular trichomes and non-glandular trichomes on the lower epidermis, and the non-glandular trichome observed in the leaf corresponds to the same type found in the stem. Cubic crystals can be observed (Figure 6).

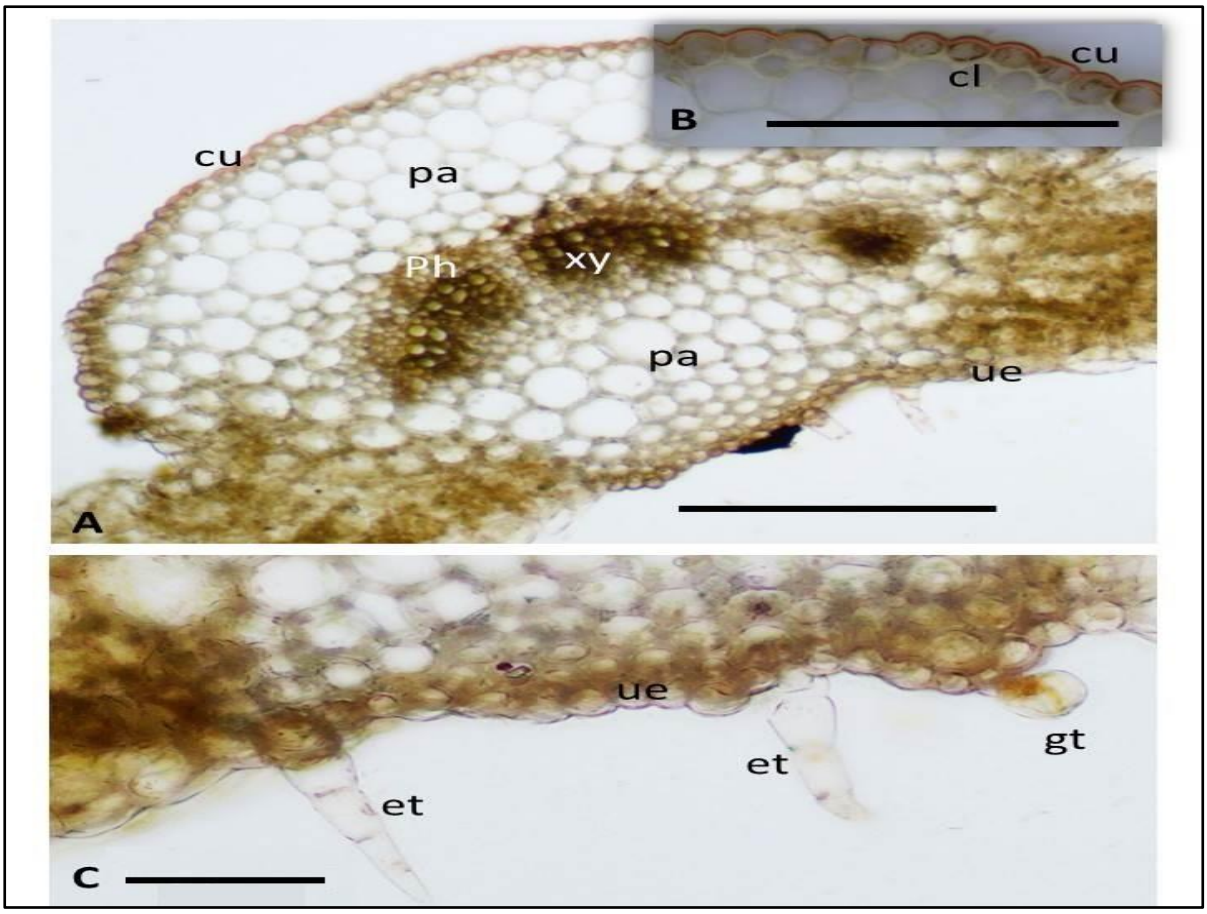

Figure 5: A) Midrib area in leaf of *O. basilicum* (scale 0.5 mm), B) Lower epidermis, C) Upper epidermis (scale 0.1 mm).
le: lower epidermis; et: eglandular trichome, pa: parenchyma, ph: phloem, xy: xylem, gt: glandular, cu: cuticle, cl: collenchyma.

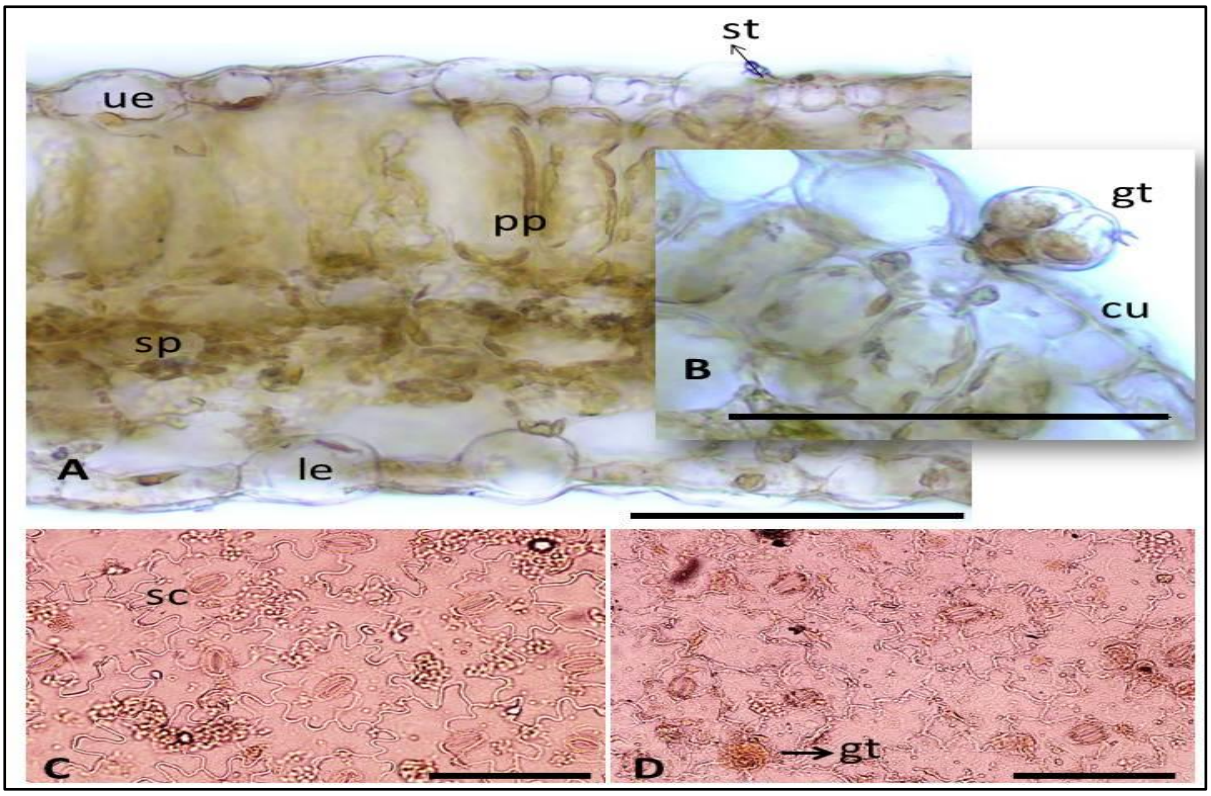

Figure 6: A) Leaf anatomy of *O. basilicum* B) Upper epidermais and glandular trichome, C) Lower epidermis, D) Upper epidermis.
ue: upper epidermis, gt: glandular trichome, le: lower epidermis, cu: cuticle, pp: palisade parenchyma,sp: spongy parenchyma, sc: stoma cell (scales: 0.1 mm).

***A. rugosa* (Fisch. & C.A.Mey.) Kuntze**

Stem anatomy

In transection, the stem presented a rectangular shape, and there is a broad pith area. The epidermis appeared in a single series with thickened and papillae cuticles. There are several layers of cells in the cortex. Beneath the epidermis, there were about 8-9 layers of angular collenchyma and 3-4 rows of oval or round shaped sponge parenchyma cells with space among them. The sclerenchyma was formed by thickened cells containing lignin, leading to a sclerenchymatous ring in the cortex. The endodermis was formed by a layer of cells around the cortex. The vascular system presented cambia, forming phloem outward and xylem inward. Druse crystals can be observed on phloem (Figure 7).

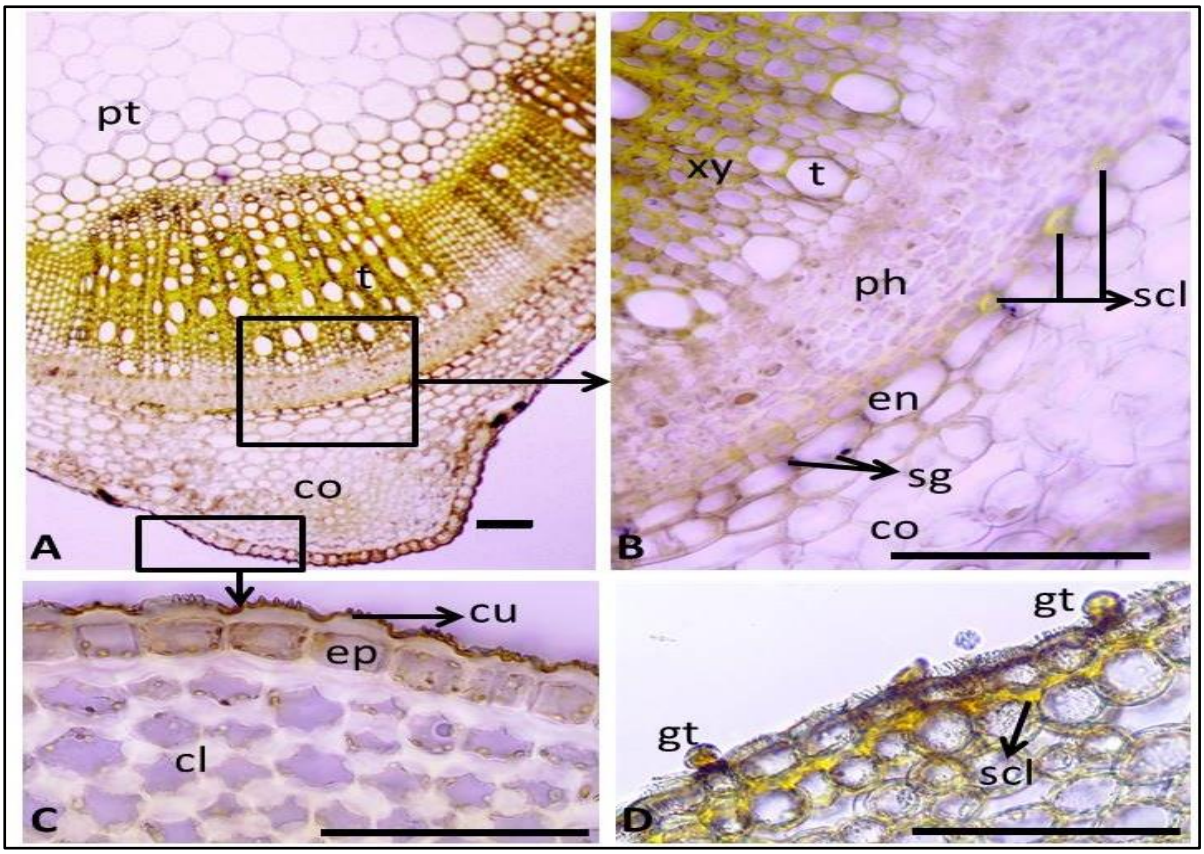

Figure 7: A) Stem anatomy of *A. rugosa*, B) Endodermis, C) Collenchyma, D) Sclerenchyma.
ep: epidermis, gt: glandular trichome, cu: cuticle, pa: parenchyma, cl: collenchyma, en: endodermis, ph: phloem, xy: xylem, t: trachea, scl: sclerenchyma, pt: pith region, co: cortex, sg: starch grains (scale 0.1 mm).

Leaf anatomy

The leaves of *A. rugosa*, in frontal view, showed epidermal cells with wavy anticlinal walls, which are relatively thin on both sides, and covered by thick and papillae cuticles. The leaves are hypostomatic. The epidermis is uniseriate. Beneath the epidermis, on both sides, there are 1-2 strata collenchyma, 2-3 layers of sclerenchyma with small round cells and 5-6 layers of parenchyma with thin walls are apparent. The vascular system was represented by an open arc, forming phloem outward and xylem inward (Figure 8). The leaves are bifacial, which contains 1-2 layers of palisade and 3-4 layers of sponge parenchyma, taking up the half mesophyll area, respectively. Druse crystals can be observed.

Only the lower epidermis of the leaves is hypostomatic and have stomata on it. The lower epidermis is composed of informal shaped cells with spaces among them, and epidermis cells of the lower surface are bigger than the upper. The anticlinal walls are wavy. Some glandular and non-glandular hairs on them. In lower epidermis stomata are diacytic type with two subsidiary cells, one is bigger than the other, and stomata are plentiful. Druse crystals can be observed on both epidermis (Figure 9).

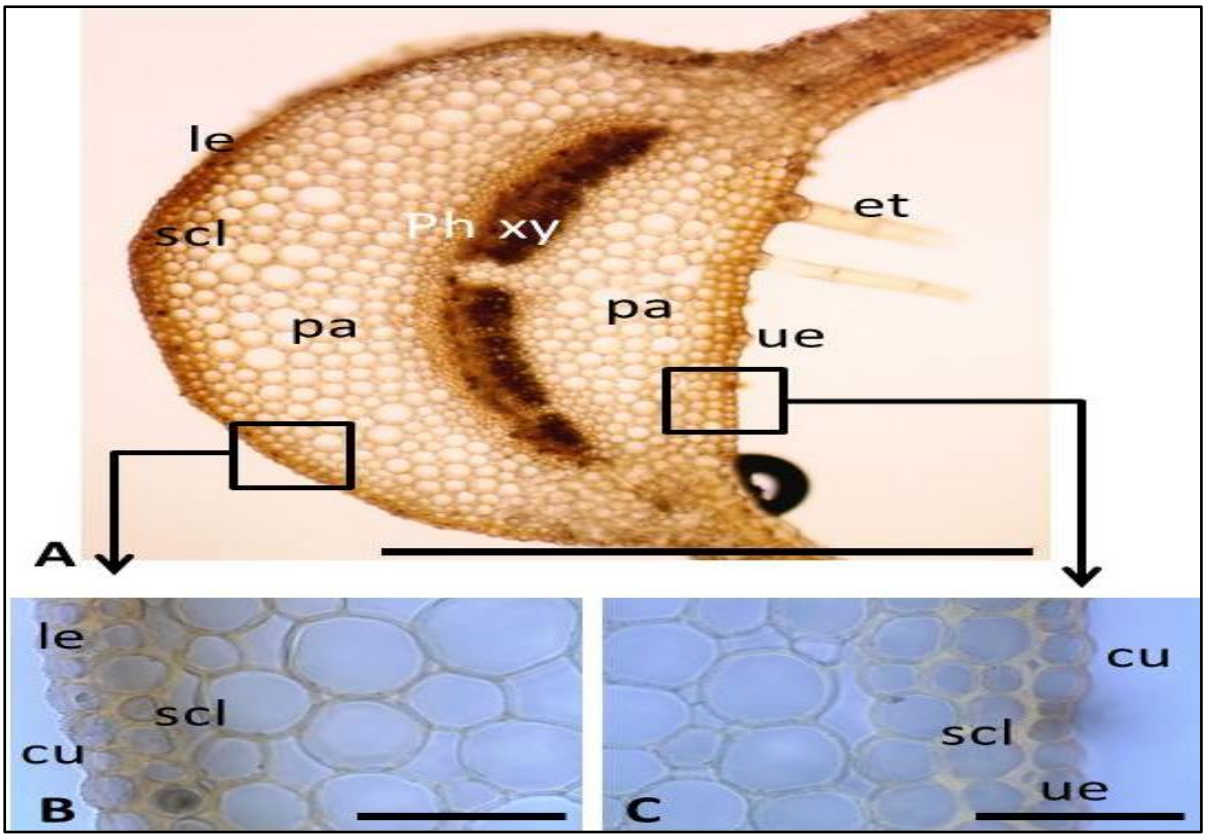

Figure 8: A) Midrib area in leaf of *A. rugosa* (scale 1 mm), B) Lower epidermis, C) Upper epidermis (scales 0.1 mm).
ue: upper epidermis, le: lower epidermis; et: eglandular trichome, pa: parenchyma, ph: phloem, xy: xylem, cu: cuticle, scl: sclerenchyma.

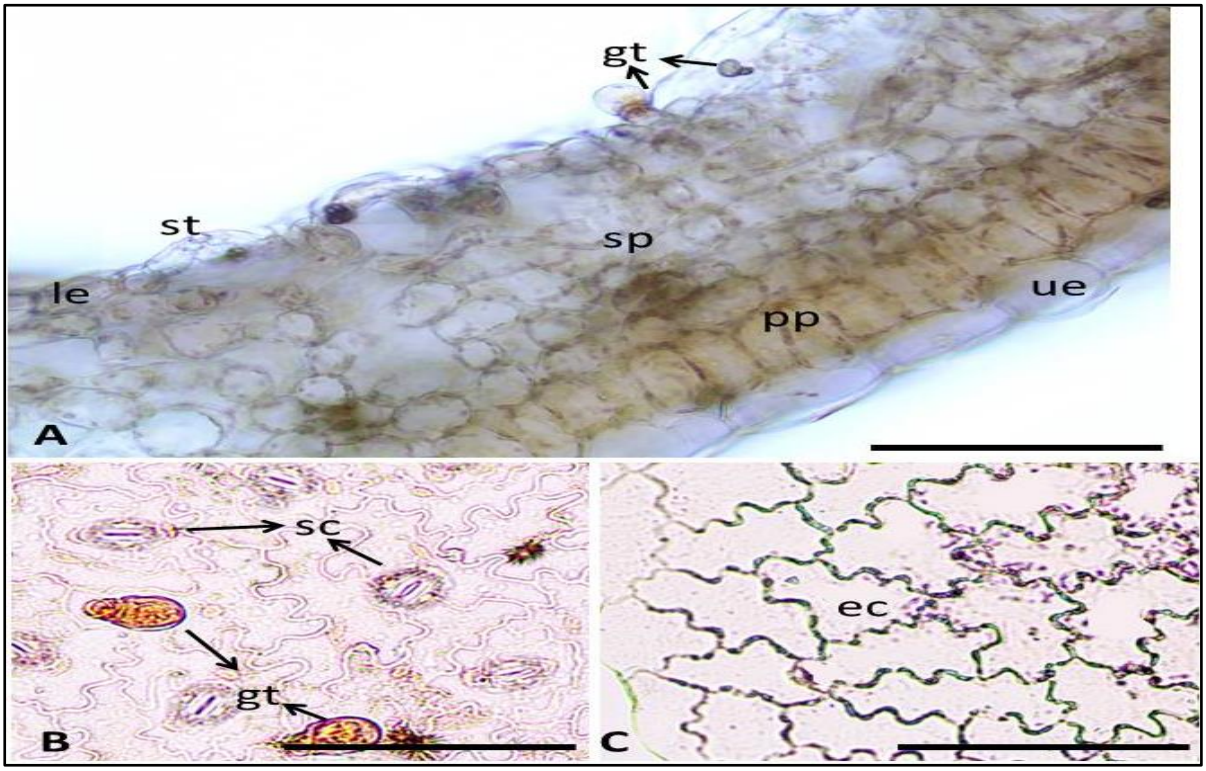

Figure 9: A) Leaf anatomy of *A. rugosa,* B) Lower epidermis, C) Upper epidermis.
ue: upper epidermis, gt: glandular trichome, le: lower epidermis, cu: cuticle, pp: palisade parenchyma, sp: spongy parenchyma, et: eglandular trichome, sc: stoma cell, ec: epidermis cell (scale 0.1 mm).

Table 1: Anatomical characteristics of *D. moldavica*, *O. basilicum* and *A. rugosa.*

	D. moldavica	***O. basilicum***	***A. rugosa***
Glandular trichome	+	+	+
Eglandular trichome	+	+	+
Crystals	-	+	+
Leaf type according to mesophyll	Bifacial	Bifacial	Bifacial
Leaf type according to stomata	Amphistomatic	Amphistomatic	Hypostomatic
Stomata types	Diacytic	Diacytic	Diacytic
Palisade layers	2	Single	Single

DISCUSSION

D. moldavica, O. basilicum and *A. rugosa* (Lamiaceae) have important medical use in cardiovascular diseases (Chinese Materia Medica, 2005; Maimaitiyiming *et al.,*2014; Huang and Liang, 1999) and always have the priority when making decoctions or preparations for the cardiovascular disorders like angina, heart palpitation, abnormal heart rhythms or coronary artery diseases (Miernisha *et al.,* 2015).

The anatomical findings of *A. rugosa* are presented for the first time in this study. Although there are no detailed anatomical studies on the other two species, anatomical studies have been carried out giving structural details such as feather structures, depot materials, growth hormones and secretory channels (Dmitruk and Weryszko-Chmielewska, 2010; Li and Ding, 2001). All anatomical findings are summarized in the table 1.

Cross sections taken from the stem of these plants have exhibited a monolayered epidermis which is composed of oval, cubic, or rectangular cells. The upper surface of epidermis is covered with a thin cuticle and contains glandular and eglandular trichomes. Eglandular trichomes are curved, simple cells made up from one to three cells and arranged in a single row containing acuticle with or without micropapillae. Capitate trichomes are small in size and either consists of a short unicellular stalk and a globose or pear-shaped head cell, or two-cellular stalks and a globose or pear-shaped head cell. Epidermis also includes diacytic stomata type. Underneath the epidermis, multilayered collenchyma cells are located at the corners and there are 1–3 rows of chlorenchyma cells between them. The parenchymatic cortex tissue consists of 7–10 layered of oval, ovate, or orbicular parenchymatous cells. The single-layered endodermis consists of generally oval cells.

In the cross section of the lamina, there is a thin cuticle on the upper and lower epidermis. Both epidermal cells are mono

layered, isodiametric, and rectangular, oval, or cubic in shape. Surface of epidermis are covered with eglandular (1–4 cells) and glandular trichomes. Stomata are present on both surfaces of the lamina (amphistomatic type) in *D. moldavica* and *O. basilicum.*

The identification of pharmaceutically used species in pharmacopeias traditionally relies, besides phytochemical characterization, on morphology and anatomy. Morphological and anatomical characteristics are thus mandatory for drugs' pharmaceutical identification and purity control. Through the comparative study of the anatomy of these three species, we hope to have furthered as well to have laid the foundation for an accurate evaluation of different sources of Lamiaceae as to ensure their safety and efficacy.

ACKNOWLEDGMENTS

We thank Scientific Research Project Unit of Istanbul University for financial support (project no. TYL-2017-25278).

REFERENCES

Aibai S (2007). Diagnosis and treatment of cardiovascular diseases treated by Uyghur Medicine. *The sixth cross-strait symp cardio*. 27-28.

Chinese Materia Medica, State Administration of Traditional Chinese Medicine (2005). Chinese herbal medicine – Volume of Uyghur medicine. Shanghai: *Shanghai science and technology Publishing Company*.

Feng ZG, Li Q (2006). Studies on chemical constituents of *Dracocephalum moldavica*. *Chin Trad Patent Med.* **1**: 94-98.

Flora of Xinjiangensis, editorial board of flora of Xinjiang. 2004. Xinjiang Science. *Technology and hygiene publishing house*.

Gong H, Li S, He L, Kasimu R (2017). Microscopic identification and in vitro activity of *Agastache rugosa* (Fisch. et Mey) from Xinjiang, China. *BMC Complement Altern Med.* **17**: 1–6.

Huang YL, Liang X (1999). Clinical observation on Treatment of Angina Pectoris of Coronary Heart Disease with Huoxiang (*Agastache rugose*) Zhengqi Powder. *Journal of Henan Traditional Chinese Medicine.* **14**(5): 51.

Li JB, Ding Y (2001). Studies on Chemical Constituents of *Dracocephalum moldavica*. *China journal of chinese materia medica***. 10**: 697-698.

Maimaitiyiming D, Hu GM, Aikemu A, Hui SW, Zhang XY (2014). the Treatment of Uyghur medicine *Dracocephalum moldavica* L. on chronic mountain sickness rat model**.** *Pharmacognosy Magazine.* **10** (40): 477-482.

Mattohti T (2015). Uyghur Medicine in Practice: A study in khotan. *Coll Antropol.* **39**: 433–436.

Miernisha A, Bi CW, Cheng LK, Xing JG, Liu J, Maiwulanjiang M, Aisa HA, Dong TT, Lin H, Huang Y, Tsim KW (2015). Badiranji Buya Keli, a traditional Uyghur medicine, induces vasodilation in rat artery: Signaling mediated by nitric oxide production in endothelial cells. *Phyther Res*. **30**(1): 16–24.

Umar A, Zhou W, Abdusalam E, Tursun A, Reyim N, Tohti I, Moore N (2014). Effect of *Ocimum basilicum* L. on cyclo-oxygenase isoforms and prostaglandins involved in thrombosis. *J Ethnopharmacol.* **152**: 151–155.

Umar A, Yimin W, Tohti I, Upur H, Berké B, Moore N (2015). Effect of traditional Uyghur medicine abnormal Savda Munziq extracts on rabbit platelet aggregation in vitro and rat arteriovenous shunt thrombosis in vivo. *J Ethnopharmacol.* **159**: 184–188.

Yi F, Hu LL, Lou FC (2004). Study on the chemical composition of *Ocimum basilicum*. *Chin J Nat Med.* **1**: 20-24.

Zhao L, Tian S, Wen E, Upur H (2017). An ethnopharmacological study of aromatic Uyghur medicinal plants in Xinjiang, China. *Pharm Biol.* **55**: 1114–1130.

Research Article EMUJPharmSci ISSN 2651-3587 https://dergipark.org.tr/emujpharmsci

EMU Journal of Pharmaceutical Sciences

EMUJPharmSci

Investigation of cholinesterase inhibitory potential of chlorinated phenols

Bahareh Noshadi, Tugba Ercetin, Acelya Mavideniz, Hayrettin Ozan Gulcan*

Eastern Mediterranean University, Faculty of Pharmacy, Famagusta, North Cyprus, Mersin 10 Turkey.

Abstract

Chlorinated phenols (i.e., totally 19 compounds from mono-chlorophenols to pentachlorophenol) have been synthesized in large amounts and used for diverse purposes within the last century. Their worldwide application in different areas also resulted in their accumulation within the environment. Therefore, it is always a topic of concern to investigate the biological effects of these compounds by various scientific disciplines, including but not limited to, toxicology, ecology, and xenobiotic metabolism. In this study, we aimed to screen the cholinesterase inhibitory potential of chlorinated phenols. The results indicated that chlorinated phenols have low to moderate potential as inhibitors of cholinesterases and the potential depends on the substitution level of phenol.

Keywords

Acetylcholinesterase, butyrylcholinesterase, chlorinated phenols, metabolism, xenobiotics.

Article History

Submitted: 23 January 2020 Accepted: 05 March 2020 Published Online: March 2020

Article Info

***Corresponding author:** H. Ozan Gulcan **e-mail:** ozan.gulcan@emu.edu.tr

Research Article:

Volume: 3 Issue: 1 March 2020 Pages: 29-34

INTRODUCTION

Chlorinated phenols consist of totally 19 compounds, representing mono-, di-, tri-, tetra-, and penta-chlorine substituted phenol analogues (Exon, 1984). Following the first identification of phenol, pentachlorophenol, and some tri-chlorophenol derivatives as fungicides, herbicides, insecticides, and antimicrobial agents, their annual production reached to enormous levels particularly after 1930s (Figure 1) (Ahlborg *et al.,* 1980; Jensen *et al.,* 1973). Beside, tetrachlorophenols were also intensively used as wood preservatives (Puhakka *et al.,* 1992). This, overall, triggered their accumulation in the environment concomitant to the questioning of their toxic effects on living things, including human (Igbinosa *et al.,* 2013). Toxicity has been also questioned related to their synthesis impurities including dibenzodioxines and dibenzofurans (Nilsson *et al.,* 1974).

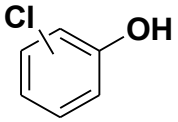

Three monochloro-, six dichloro-, six trichloro-, three tetrachloro-, and one pentachloro substituted phenol analogues

Figure 1: The general structure of chlorinated phenols.

Today, beside occupational exposure, living things are exposed to these compounds from various sources including water (Lampi *et al.,* 1990). Therefore, the metabolism aspect of these compounds have been investigated in detail. These compounds, in general have diverse tissue distribution including liver and kidney (Wagner *et al.,* 1991). Although majority of the pharmacokinetic studies depend on the results obtained for pentachlorophenol, in general many of these compounds have been shown to be eliminated from the organism in less than 24 hours (Nikkilä *et al.,* 2003). In terms of metabolic pathways, the studies indicated particularly the interaction of these compounds with Cyp450 enzymes, resulting in the production of oxidative dechlorination products. These are either quinone or more hydroxylated phenol derivatives (Mehmood *et al.,* 1996). Beside the metabolism in human, nature also directs the degradation of these compounds in soil through microorganisms ending up with mono-chlorinated derivatives (Murthy *et al.,* 1979). Regarding their importance with respect to exposure from the environment, there has always been interest to investigate the interaction of these compounds with different biological cascades (Gulcan *et al.,* 2008). From this perspective, in this study, we aimed to screen the potential of chlorinated phenols

to inhibit cholinesterase enzymes (i.e., acetylcholinesterase (AChE), and butyrylcholinesterase (BuChE)).

MATERIALS AND METHODS

The chlorinated phenol derivatives were obtained from Sigma Aldrich (CA, USA). Their purities were more than 99 % as stated on their labels. Therefore, no other purification was conducted on the reagents.

Determ*ination of AChE and BChE inhibitory activities*

The modified spectrophotometric method of Ellman was used to determine of AChE and BuChE inhibitory activities of the chlorinated phenols (Gulcan *et al.,* 2014). The enzymes used for cholinesterase activity studies were electric eel AChE (eeAChE) (Sigma) and equine BuChE (Sigma).

Acetylthiocholine iodide and butyrylthiocholine chloride (Sigma, St. Louis, MO, USA) were employed as substrates of the reaction. 5, 5′-Dithio-bis (2-nitrobenzoic) acid (DTNB, Sigma, St. Louis, MO, USA) was used for the measurement of the cholinesterase activity. Briefly, 50 mM Tris HCl buffer (pH 8.0), 6.8 mM DTNB, 2 µl of sample solutions and 10 µl of AChE/BChE solution were added in a 96-well microplate. The reaction was then initiated with the addition of 10 µl of acetylthiocholine iodide/butyrylthiocholine chloride. The hydrolysis of acetylthiocholine iodide/butyrylthiocholine chloride was monitored at a wavelength of 412 nm by the formation of the yellow 5-thio-2-nitrobenzoate anion as a result of the reaction of DTNB with thiocholines at 27°C for 5 min, catalyzed by enzymes (Varioskan Flash, Thermo Scientific, USA). The measurements and calculations were evaluated by using SkanIt Software 2.4.5 RE for Varioskan Flash software. Percentage of inhibition of AChE and BuChE was determined by comparing the rates of reaction of samples relative to blank sample (methanol) using the formula (E-S)/E x 100, where E is the activity of enzyme without test sample and S is the activity of enzyme with test sample. The experiments were done in triplicate. Donepezil hydrochloride, and rivastigmine were used as reference compounds. The percent inhibition at 100 and 50 µM was obtained for each test compound with standard compounds.

RESULTS AND DISCUSSION

The activities obtained for the potential of chlorinated phenol derivatives to inhibit cholinesterase enzymes are shown in Table 1. Accordingly, the compounds displayed varying activities depending on the chlorine substitution pattern.

First of all, the inhibition potential of each compound was found to be concentration dependent. In other words, the potential of the compounds to inhibit both cholinesterase enzymes were measured higher with the increasing concentration. On the other hand, the compounds were found more active on AChE, and their potential on the inhibition of BuChE was found lower for almost each compound analyzed.

Small variances were observed within the group of compounds possessing the same number of chlorine substitutions. The average inhibition percentage of mono-chlorinated phenols was found lower in comparison to the rest of the compounds. However, the increase in the potential to inhibit the cholinesterase enzymes corresponding to the number of chlorine substitutions was too different from di-chlorine substituted derivatives to the tetra-substituted analogues, although the average percent inhibition depending on the group of compounds possessing the same of number of chlorine substitution was found to be almost the same.

The highest activity was observed for pentachlorophenol for the inhibition of AChE, while its BuChE inhibition was found almost identical for each of other molecules analyzed.

There is limited data on the investigation of chlorinated phenols with respect to their interaction with cholinesterases (Klemmer *et al.,* 1980; Igisu *et al.,* 1993). From this perspective, the study presented here, for the first time, have indicated the potential of chlorinated phenols to act as cholinesterase inhibitors. Overall, the activities of phenol compounds were found quite low to be further analyzed with respect to the metabolism and toxicological perspectives. Indeed, the concentrations employed within this study are relatively high for acute exposure conditions. However, the potential of the compounds obtained might be evaluated from the occupational or environmental perspectives leading to the chronic exposure to one of these compounds.

Table 1: The potential the title compounds to inhibit AChE and BuChE enzymes.

Chlorinated phenols	% Inhibition (AChE) 50µM	% Inhibition (AChE) 100µM	% Inhibition (BuChE) 50µM	% Inhibition (BuChE) 100µM
2-chlorophenol	9.6 ± 0.3	19.0 ± 0.1	5.2 ± 0.2	9.2 ± 0.7
3-chlorophenol	5.1 ± 0.4	22.1 ± 0.3	4.3 ± 0.9	7.0 ± 0.5
4-chlorophenol	4.7 ± 0.3	18.7 ± 0.2	4.6 ± 0.1	7.3 ± 0.5
2,3-dichlorophenol	14.5 ± 0.1	21.5 ± 0.4	8.2 ± 0.5	11.3 ± 0.4
2,4-dichlorophenol	11.0 ± 0.1	28.3 ± 0.7	6.1 ± 0.2	9.3 ± 0.2
2,5-dichlorophenol	15.0 ± 0.37	27.1 ± 0.9	5.0 ± 0.5	8.3 ± 0.2
2,6-dichlorophenol	12.2 ± 0.7	30.2 ± 0.1	7.3 ± 0.4	10.1 ± 0.1
3,4-dichlorophenol	10.1 ± 0.5	31.1 ± 0.3	7.2 ± 0.1	9.8 ± 0.3
3,5-dichlorophenol	18.2 ± 0.4	25.2 ± 0.2	8.4 ± 0.2	11.3 ± 0.1
2,3,4-trichlorophenol	9.5 ± 0.3	18.3 ± 0.2	7.5 ± 0.2	8.1 ± 0.2
2,3,5-trichlorophenol	16.4 ± 0.5	27.0 ± 0.9	5.4 ± 0.1	8.0 ± 0.1
2,3,6-trichlorophenol	17.7 ± 0.4	25.2 ± 0.6	7.0 ± 0.6	10.3 ± 0.8
2,4,5-trichlorophenol	10.7 ± 0.3	30.3 ± 0.1	5.5 ± 0.1	10.7 ± 0.9
2,4,6-trichlorophenol	8.4 ± 0.1	20.0 ± 0.5	4.5 ± 0.5	11.9 ± 0.1
3,4,5-trichlorophenol	9.3 ± 0.5	19.7 ± 0.8	3.9 ± 0.2	10.3 ± 0.4
2,3,4,5-tetrachlorophenol	14.2 ± 0.6	35.2 ± 0.5	4.1 ± 0.5	14.2 ± 0.6
2,3,4,6-tetrachlorophenol	14.0 ± 0.3	37.3 ± 0.4	4.5 ± 0.6	9.0 ± 0.3
2,3,5,6-tetrachlorophenol	17.0 ± 0. 7	33.3 ± 0.2	6.1 ± 0.9	13.8 ± 0.7
Pentachlorophenol	19.0 ± 0.1	38.1 ± 0.4	7.0 ± 0.4	13.9 ± 0.2
Donepezil	89.0 ± 0.8	92.3 ± 0.9	83.2 ± 0.5	87.2 ± 0.9
Rivastigmine	69.9 ± 0.2	79.1 ± 0.3	78.8 ± 1.1	81.3 ± 0.5

CONCLUSION

It is apparent that the research on the investigation of environmentally exposured compounds and their activities inside the organisms has always been a topic of concern. In this study, the potential of chlorinated phenols to act as cholinesterase inhibitors was investigated and it was concluded that these molecules have negligible significance in terms of a side or toxic effect with respect to cholinesterase inhibition. However, the low potential must be at the same time evaluated depending on the acute/chronic exposure concomitant to the presence of other molecules.

REFERENCES

Ahlborg UG, Thunberg TM, Spencer HC (1980). Chlorinated phenols: occurrence, toxicity, metabolism, and environmental impact. *CRC Crit Rev Toxicol.* **7**(1): 1-35.

Exon JH (1984). A review of chlorinated phenols. *Vet Hum Toxicol.* **26**(6): 508-520.

Gulcan HO, Liu Y, Duffel MW (2008). Pentachlorophenol and other chlorinated phenols are substrates for human hydroxysteroid sulfotransferase hSULT2A1. *Chem Res Toxicol.* **21**(8): 1503-1508.

Gulcan HO, Unlu S, Esiringu I, Ercetin T, Sahin Y, Oz D, Sahin MF (2014). Design, synthesis and biological evaluation of novel 6H-benzo [c] chromen-6-one, and 7, 8, 9, 10-tetrahydro-benzo [c] chromen-6-one derivatives as potential cholinesterase inhibitors. *Bioorg Med Chem.* **22**(19): 5141-5154.

Igbinosa EO, Odjadjare EE, Chigor VN, Igbinosa IH, Emoghene AO, Ekhaise FO, Idemudia OG (2013). Toxicological profile of chlorophenols and their derivatives in the environment: the public health perspective. *Sci World J.*

Igisu H, Hamasaki N, Ikeda M (1993). Highly cooperative inhibition of acetylcholinesterase by pentachlorophenol in human erythrocytes. *Biochem Pharmacol* **46**(1): 175-177.

Jensen S, Renberg L (1973). Chlorinated dimers present in several technical chlorophenols used as fungicides. *Environ Health Perspect.* **5**: 37-39.

Klemmer HW, Wong L, Sato MM, Reichert EL, Korsak RJ, Rashad MN (1980). Clinical findings in workers exposed to pentachlorophenol. *Arch Environ Contam Toxicol.* **9**(6): 715-725.

Lampi P, Vartiainen T, Tuomisto J, Hesso A (1990). Population exposure to chlorophenols, dibenzo-p-dioxins and dibenzofurans after a prolonged ground water pollution by chlorophenols. *Chemosphere* **20**(6): 625-634.

Mehmood Z, Williamson MP, Kelly DE, Kelly SL (1996). Metabolism of organochlorine pesticides: the role of human cytochrome P450 3A4. *Chemosphere* **33**(4): 759-769.

Murthy NBK, Kaufman DD, Fries GF (1979). Degradation of pentachlorophenol (PCP) in aerobic and anaerobic soil. *J Environ Sci Health B.* **14**(1): 1-14.

Nikkilä A, Halme A, Kukkonen JV (2003). Toxicokinetics, toxicity and lethal body residues of two chlorophenols in the oligochaete worm, Lumbriculus variegatus, in different sediments. *Chemosphere* **51**(1): 35-46.

Nilsson CA, Renberg L (1974). Further studies on impurities in chlorophenols. *J Chromatogr A* **89**(2): 325-333.

Puhakka JA, Järvinen K (1992). Aerobic fluidized-bed treatment of polychlorinated phenolic wood preservative constituents. *Water Res.* **26**(6): 765-770.

Wagner SL, Durand LR, Inman RD, Kiigemagi U, Deinzer ML (1991). Residues of pentachlorophenol and other chlorinated contaminants in human tissues: Analysis by electron capture gas chromatography and electron capture negative ion mass spectrometry. *Arch Environ Contam Toxicol.* **21**(4): 596-606.

Research Article EMUJPharmSci ISSN 2651-3587 https://dergipark.org.tr/emujpharmsci

EMU Journal of Pharmaceutical Sciences

EMUJPharmSci

Development of an effervescent tablet formulation which contains ferrous salt and ascorbic acid combination

Hasip Cem Ozyurt*, Reza Mehrad

Eastern Mediterranean University, Faculty of Pharmacy, Famagusta, North Cyprus, Mersin 10 Turkey.

Abstract

This study aimed to develop the formulation of effervescent tablets containing ferrous sulfate and ascorbic acid combination to increase intestinal iron absorption and reduce gastrointestinal side effects related to iron supplementation.

In this study, the prototype formulation was calculated precisely and then prepared by three different methods for compression and evaluation. The flowability of powders and granules was investigated. Effervescent tablets were produced by direct compression and two different wet granulation methods. The produced tablets were then evaluated for acceptable hardness, friability <1 %, effervescence time <5 minutes, solution pH <6, water content <0.5 %, and optimum content uniformity.

The powder mixture prepared for the direct compression method had acceptable flowability but required a high compression force. Flowability and other physicochemical properties of this powder, including compressibility and hardness, were improved by granulation. The taste and color of the effervescent solution had good acceptability for the volunteers.

The results of the effervescent tablets produced by the GM2 method, which contain a higher percentage of granulated content were better than the other two methods. The PVP binder solution is suitable to produce effervescent granules that are compressed into tablets, due to improvements in flowability and compactibility.

Keywords

Direct compression method, effervescent tablets, ferrous sulfate, iron deficiency, wet granulation method

Article History

Submitted: 10 February 2020 Accepted: 04 March 2020 Published Online: March 2020

Article Info

***Corresponding author:** Hasip Cem Ozyurt **e-mail:**cem.ozyurt@emu.edu.tr

Research Article:

Volume: 3 Issue: 1 March 2020 Pages: 35-49

INTRODUCTION

Effervescents consist of a soluble organic acid and an alkali metal carbonate salt that release carbon dioxide in contact with water. Effervescent tablets are usually made by compressing the active ingredients with a mixture of sodium bicarbonate and organic acids, such as citric acid and tartaric acid (Lachman *et al.,* 1986).

In general, these tablets contain drugs that dissolve quickly upon entry into the water and are recommended as a clear, palatable solution (Allen *et al.,* 2011). Therefore, they can be prescribed for patients suffering from swallowing tablets or capsules (Swarbrick and Boylan, 2002). The main advantage of effervescent tablets is the fast onset of action due to the quick production of buffered effervescent solution (Altomare *et al.,* 1997).

Excipients such as water-soluble lubricants (e.g., PEG 6000 and sodium benzoate), sweeteners, flavors, and pharmaceutical dyes (Mohrle, 1989), polyvinylpyrrolidone K-30 is an effective binder for effervescent tablets and can be used both in wet granulation and in direct compression (Callahan *et al.,* 1982; Mohrle, 1989).

Low relative humidity (maximum 25 % or less) and moderate to cool temperatures (25 °C) in the manufacturing areas are essential to prevent granules or tablets from sticking to the machinery and from picking up moisture in the air, which may cause product degradation (Mohrle, 1989).

In direct compression manufacturing method, powder mixtures with excellent flowability without particle segregation are required, and the particle size of all raw materials should be equal. Granulation is necessary when the particle size is small (Saleh *et al.,* 1988; Swarbrick and Boylan, 2002). The granulating fluids, which are being used, are non-reactive solutions containing ethanol or isopropanol, in which most of the tablet components are insoluble (Mohrle, 1989).

Effervescent tablets are manufactured and controlled in the same way as conventional tablets. These quality controls include physicochemical properties such as hardness, weight variation, friability, dissolution time, pH, and content uniformity (Mohrle, 1989).

Anhydrous ferrous sulfate ($FeSO_4$) is an odorless greyish-white powder. It is slowly but almost completely soluble in water and practically insoluble in ethanol. Relative molecular mass for the anhydrous form of $FeSO_4$ is 151.91 g/mol (WHO, 2019).

$FeSO_4$ supplements are prescribed for conditions such as iron deficiency, pregnancy, heavy menstrual periods, prevention and treatment of anemia, blood

loss, frequent blood donors, hemodialysis patients, and following gastrectomy or intestinal resection (Boccio and Iyengar, 2003).

Although oral products containing ferrous sulfate in various dosage forms such as capsules, tablets, chewable tablets, syrup, suspension, and elixir are available in the pharmaceutical market, patients are reluctant to continue taking them due to gastrointestinal side effects such as constipation, stomachache, nausea and vomiting, change in color of stool, metallic taste, and diarrhea (Tolkien *et al.,* 2015). These patients have to take vitamin C supplements at the same time to increase iron absorption and minimize the side effects of taking them.

Until now, in the pharmaceutical market especially in Turkey and Iran, an effervescent tablet that provides 100 % of iron RDA (18 mg/day) in combination with a high dose of ascorbic acid (500 mg) was not produced. Therefore, this is a new and functional study.

The aim of this study was to design, develope and evaluation of the effervescent tablets, which contain ferrous sulfate and ascorbic acid combination.

MATERIALS AND METHODS

Chemicals

Sodium bicarbonate (EMBOY), citric acid monohydrate (Sigma-Aldrich®), ascorbic acid (ZAG Kimya®), PVP K-30 (ZAG Kimya®), sodium benzoate (Mediko Kimya), aspartame (Amino Sweet®), sucrose (Alfa Aesar®), lactose monohydrate (Sigma-Aldrich®), polyethylene glycol 6000 (Merck KGaA), isopropyl alcohol 99.7 % (emirkimya) and saccharin (Sigma-Aldrich®) were supplied by Eastern Mediterranean University Pharmaceutical Department. Ferrous sulfate heptahydrate (FreyBG), red powder food colorant (Chefmaster®), and lemon aroma (Scrapcooking®) were purchased from a Chinese supplier.

Pre-formulation Studies and Prototype Formulation Development

Among the food acids, citric acid is more preferred because it is widely available and relatively inexpensive, has excellent solubility and a pleasant taste. It is very hygroscopic and must be used with caution to prevent exposure to moisture during manufacturing and storage. Sodium bicarbonate is the most commonly used carbonate source because it is completely soluble in water, non-hygroscopic, inexpensive and abundant (Mitul, 2010; Mohrle, 1989).

The stoichiometric ratio between the effervescent ingredients is 1:1.3 for the citric acid anhydrous:sodium bicarbonate.

However, it is advisable to leave a small amount of citric acid unreacted to enhance palatability and taste (Allen *et al.,* 2011).

Ferrous sulfate is suitable for the formulation of effervescent tablets because of its water solubility and high elemental iron content. Ascorbic acid should be added to the formulation due to its reducing properties that cause a stabilizing effect on the iron-II salt. The recommended daily allowance (RDA) for elemental iron depends on a person's age and sex but generally for adults is 18 mg/day (Heinrich, 1974).

The diluents used should be highly water-soluble, have a particle size in the range of other effervescent ingredients, and possess excellent compressibility. Diluents may also be selected from lactose, mannitol, sorbitol, or mixtures thereof, and spray-dried lactose is also commonly used. Spray-dried lactose is particularly preferred because it facilitates the blend flowability and thus improves compressibility and tableting of the formulation (Mitul, 2010; Mohrle, 1989).

Water-soluble binders are necessary for effervescent tablets to bring the tablet hardness to a point where handling is possible. However, binder levels should be kept to a minimum to avoid delay of disintegration. PVP K-30 is an effective binder for effervescent tablets, as it dissolves rapidly in water and forms a clear solution. It is suitable for wet granulation method and direct compression. It can be used in wet granulation processes in two ways, dissolved in a granulating liquid (isopropyl alcohol) as a binder solution or added to powder blends in dry form and then granulated (Hadisoewignyo *et al.,* 2016; Kasperek *et al.,* 2016; Mohrle, 1989).

Lubricants such as magnesium stearate are not used because their water insolubility results in cloudy solutions and extended disintegration times. Spray-dried leucine and PEG are water-soluble alternatives. The micronized polyethylene glycol 6000 was prepared by freezing PEG 6000 before grinding to make it brittle and then added to the formulated mixture in the final step prior to the tableting. PEG 6000 has a low melting point of 55-63 °C, so it should be added to precooled granules to prevent stickiness problem (Conway, 2008; Rowe *et al.,* 2009).

Both artificial and natural sweeteners are used. However, in most formulations, sodium cyclamate is used in combination with saccharin sodium to mask the off-tastes of both sweeteners, often in a ratio of 10:1 (Conway, 2008; Rowe *et al.,* 2009). Water-soluble flavoring agent in dry form should be used in the formulation. Flavors such as mint, lemon or orange can help mask a bitter or metallic

taste in the mouth (Conway, 2008; Mohrle, 1989).

All ingredients must be converted to anhydrous form to prevent the components within the formulation from reacting with each other during storage. Therefore, citric acid monohydrate and ferrous sulfate heptahydrate were heated to lose their water of crystallization using the oven until they reached a constant weight. Citric acid monohydrate can be converted to the anhydrous form at about 78 °C. Ferrous sulfate heptahydrate green crystals lost their crystallization water after drying at 150 °C for 10 hours and turned to a brown-colored anhydrous solid (Conway, 2008; Heinrich, 1974). The prototype formulation was first calculated for the 2000 mg tablets, and then the formulation materials were mixed and granulated. Afterward, the prepared granules were compressed using a tablet press machine (ERWEKA EP-1) with a 20 mm diameter punch. The pressed tablets were evaluated for their weight, thickness, and hardness using an electronic balance and ERWEKA (TBH 125) hardness tester. According to the results, the tableting machine was adjusted to obtain the desired tablet thickness, hardness, and weight. Finally, the formulation was modified based on the average tablet weight (Ozyurt and Evcin, 1994; Ozyurt and Evcin, 1994).

Methods of Production

Direct Compression

The formulation materials were weighed according to Table 1, then sodium bicarbonate was dried at 100 °C for 1 hour and mixed with the other components for 15 minutes. After preparing the primary mixture, saccharin sodium sweetener and lemon flavor were passed through a 0.8 mm sieve and added to the mixture and mixed for 5 minutes. Finally, the PEG 6000 lubricant was added and mixed with other materials for about 2-5 minutes again. The powder mixture was then compressed into tablets using a tablet press machine (ERWEKA EP-1) with a 20 mm punch at a maximum of 25 % RH. In the end, the tablets were dried in an oven with air circulation at 50 °C for 1 hour and then packed in plastic tubes after cooling. Figure 1 shows direct compression of ferrous sulfate plus ascorbic acid effervescent tablets.

Table 1: Prototype formulation of ferrous sulfate and ascorbic acid combination based on preformulation studies.

Mixture or Solution	Material Name	Tested Concentrations (%)	Selected Concentration (%)	mg/tablet
I.	Sodium bicarbonate	25-50	25	500
	Citric acid anhydrous (powder)	10-22.5	21.5	430
	Red dye	0.1-0.5	0.3	6
II.	Povidone, PVP K30	0.5-5	0.5	10
	Isopropanol	q.s.*	q.s.*	0.20 mL
III.	Ascorbic acid (powder)	25	25	500
	Ferrous sulfate anhydrous (powder)	2.5	2.5	50
	Sucrose (fine crystals)/Lactose anhydrous	q.s.*	21.87	438
IV.	Lemon flavor	0.03-0.5	0.03	0.6
	Saccharin sodium	0.075-0.6	0.05	1
V.	Micronized PEG 6000	2-5	3.25	65

*q.s: quantum sufficit

Figure 1: Direct compression of ferrous sulfate plus ascorbic acid effervescent tablets.

Wet Granulation Method

Wet granulation was performed using two different procedures.

1- According to Table 1, mixture I was passed through 35 mesh sieve (<0.5 mm) and blended for 10 minutes. Then, 5 % w/v PVP K-30 solution in isopropanol was added dropwise using a pipette to the mixture until an orange pasty mass formed. This wet mass was passed through sieve No. 10, and the resulting granules were dried in an oven at 50 °C until dry. The dried mass was then passed through 10 mesh sieve. Mixture III was also dried at 60 °C and mixed with the granule mass and mixture IV for 5 minutes. At last, the PEG 6000 lubricant was added to other materials and mixed for 2-5 minutes. The granule mixture was compressed into tablets using a tablet press machine (ERWEKA EP-1) with a 20 mm punch at a maximum of 25 % RH. The prepared tablets were dried in an oven with air circulation at 50 °C for 90 minutes, then covered with aluminum foil and packed in plastic tubes. Tableting of granules produced by wet granulation method-1 is shown in Figure 2.

Figure 2: Tableting of granules produced by wet granulation method-1.

Figure 3: Tableting of granules produced by wet granulation method-2.

2- In this method, the active ingredients were mixed with acid and base and then granulated with the binder solution. That is, mixtures I and III were first blended, and then granulated with solution II in the same manner explained. The resulting granules were then dried and mixed with mixture IV. At the last step, by adding lubricant, the granule mixture was prepared for the tableting process (Figure 3). Better results were observed when lactose anhydrous was used instead of sucrose in this method.

Evaluation of Pre-compression Parameters

Angle of Repose

The angle of repose was measured by the fixed funnel method. Approximately 10 g of granule or powder was poured through a funnel that was fixed at a certain height (10 cm) above graph paper. The diameter (D) and the height of the formed cone (h) were measured to calculate the angle of repose (θ) using the following trigonometric relationship (Aulton and Taylor, 2013):

$$\text{Angle of Repose } (\theta) = \tan^{-1}\left[\frac{\text{height of the heap (h)}}{0.5 \times \text{diameter of the base (D)}}\right]$$

This test was repeated three times for each method, and the mean of three measurements was interpreted (USP31–NF26, 2008).

Carr's Compressibility Index and Hausner Ratio

These terms describe the flow properties of powders. The compressibility index is expressed in percentage and calculated by the following equation (Ashish *et al.,* 2011; Aulton and Taylor, 2013):

$$\text{Compressibility Index} = 100 \times \left[\frac{\text{tapped density (}\rho\text{ tapped)} - \text{bulk density (}\rho\text{ bulk)}}{\text{tapped density (}\rho\text{ tapped)}}\right]$$

The Hausner ratio was calculated from the following equation (Ashish *et al.,* 2011):

$$\text{Hausner Ratio} = \frac{\text{tapped density (}\rho\text{ tapped)}}{\text{bulk density (}\rho\text{ bulk)}}$$

Compressibility Index and Hausner ratio parameters were obtained using the mean

of three measurements of ρ bulk and ρ tapped and compared (USP31–NF26, 2008).

Bulk Density

To measure bulk density, a quantity of accurately weighed granules and powders (100 g) was poured into the graduated cylinder (250 mL) using a funnel without compacting, and then its volume was recorded. Bulk density is expressed in grams per milliliter and calculated by the following formula (Aulton and Taylor, 2013; Palanisamy *et al.,* 2011):

$$\text{Bulk Density } (\rho\text{bulk}) = \frac{\text{weight of powder (m)}}{\text{volume of powder (V bulk)}}$$

Tapped Density

After measuring bulk density, the cylinder was tapped from a height of 2.5 cm until powder volume remained constant. Tapped density was calculated from the following formula (Remington, 2011):

$$\text{Tapped Density } (\rho\text{tapped}) = \frac{\text{weight of powder (m)}}{\text{minimum volume occupied after tapping (V tapped)}}$$

Determination of Particle Size Distribution

The mean particle size of the granules was determined by the sieving method. Selected sieves with different meshes (18, 35, 60, 120) were placed on the sieve shaker. 100 g of granules were placed on the upper sieve. After 10 minutes of shaking, the amount of granule retained on each sieve was weighed. The mean diameter of powders was calculated by the following equation (Moghimipour *et al.,* 2010; Yanze *et al.,* 2000):

$$\text{Mean Particle Diameter (d)} = \frac{\Sigma x_i d_i}{100}$$

x_i = The average size of both the upper and lower sieve

d_i = The percentage of the value i in that range of bulk.

Evaluation of Post-compression Parameters

Tablet Dimensions

Thickness and diameter of 10 tablets from each method were measured using a micrometer. The mean deviation of

thickness should not exceed 5 % of its acceptable limits (Lachman *et al.,* 1986).

Hardness

Tablet hardness was measured for 10 tablets of each method using the ERWEKA (TBH 125) hardness tester, and the average hardness was calculated. The hardness of effervescent tablets is usually lower than that of conventional tablets, and the minimum acceptable hardness for uncoated tablets is approximately 40 N (Patel and Chauhan, 2012).

Uniformity of Weight

Twenty tablets of each method were weighed individually using an analytical balance and the average weight was calculated. According to the EP for tablets

with average weight more than 250 mg, not more than two tablets can deviate 5 % from the average weight and none deviates by more than twice that percentage (Aslani and Fattahi, 2013).

Friability

A total of 20 tablets of each method were weighed together and placed in the ERWEKA friability tester and then rotated at 25 rpm for 4 minutes. The tablets were then re-weighed and the percentage loss calculated from the following equation (Aslani and Sharifian, 2014); If weight loss is not greater than 1 %, it is acceptable (Lachman *et al.,* 1986).

$$\% \text{ Friability} = \frac{\text{Weight of tablets before test} - \text{Weight after test}}{\text{Weight of tablets before test}} \times 100$$

Disintegration Time Measurement

One tablet was dissolved in a beaker containing 200 mL of purified water at 15-25 °C, and the effervescent time was measured using a stopwatch. Whenever a clear, particle-free solution was obtained, the effervescence time has finished. The average of six measurements was calculated for each method (WHO, 2019).

Effervescent Solution pH

One tablet was dissolved in 200 mL of purified water at 20±1 °C. Immediately after completing dissolution, the solution pH was measured using a pH meter. This test was repeated three times for each method (Aslani and Fattahi, 2013).

Water Content

A total of 10 tablets of each formulation were weighed before and after drying in a desiccator containing activated silica gel for 4 hours. The percentage of their water content was calculated from the following equation (Aslani and Sharifian, 2014); The water content of 0.5 % or less is acceptable (Yanze *et al.,* 2000).

$$\text{Water content} = \frac{\text{weight before drying} - \text{weight after drying}}{\text{weight before drying}} \times 100$$

CO_2 Content

One effervescent tablet was dissolved in 100 mL of 1 N sulfuric acid solution, and weight changes were determined after the dissolution completed. The obtained weight difference showed the amount (mg) of CO_2 per tablet. The average of 3 determinations was calculated for each method (Moghimipour *et al.,* 2010).

Assay

First, 14 effervescent tablets of dried ferrous sulfate were triturated, and the crushed powder containing 700 mg of anhydrous ferrous sulfate was weighed and dissolved in a mixture of 20 mL of water and 20 mL of dilute sulfuric acid, then 2 mL of phosphoric acid was added. This solution is immediately titrated against 0.02 M potassium permanganate VS to a

pink endpoint. Each mL of 0.02 M potassium permanganate VS is equal to 15.1908 mg of anhydrous ferrous sulfate (Japanese Pharmacopoeia, 2002).

Uniformity of Content

10 tablets of each manufacturing method were selected randomly to determine the amount of active ingredient by the method described in the assay and calculate the amount of active ingredient per tablet. The acceptance limits are 94.3-105.8 % for 10 sample tablets (USP26, 2002).

RESULTS

The preformulation study results showed that the optimum stoichiometric ratio is 1:1.3 for the citric acid: sodium bicarbonate that produces a clear effervescent solution in the shortest effervescent time. The amount of ferrous sulfate anhydrous per tablet should be considered 50 mg equal to 18 mg of elemental iron that is recommended daily allowance of iron for adults.

The pre-compression evaluation results for parameters including angle of repose, compressibility index, Hausner ratio, and particle size distribution are presented in Table 2 and Figure 4.

Table 2: Pre-compression evaluation of blends.

Flowability Tests	Methods GM1	GM2	D
Angle of Repose	23.01	22.73	26.42
Compressibility Index (%)	10	8.57	22.22
Hausner Ratio	1.11	1.09	1.28

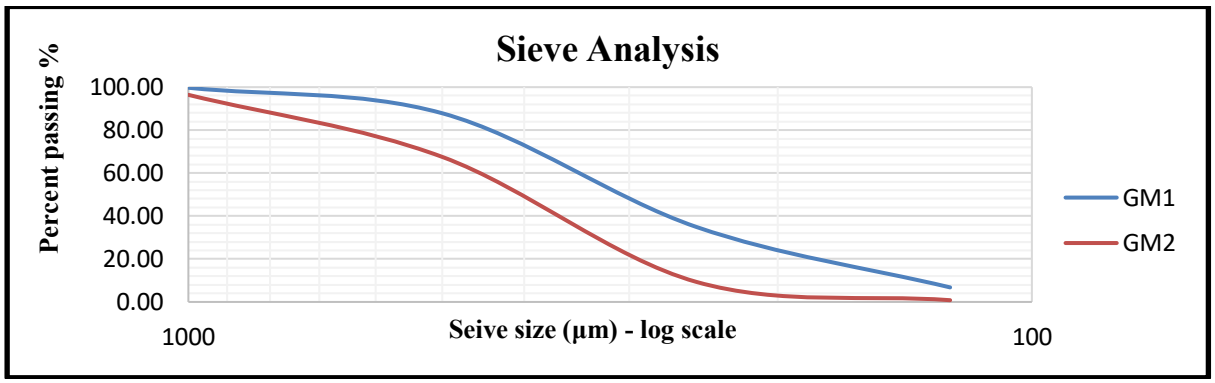

Figure 4: Particle size distribution graph of the formulation in wet granulation methods.

The post-compression evaluation results for parameters such as tablet thickness, diameter, hardness, friability, weight, variation, effervescence time, pH of the solution, moisture and CO_2 content, and content uniformity are presented in Table 3.

Table 3: Post-compression evaluation of produced effervescent tablets.

QC Tests for Effervescent Tablets	Methods		
	GM1	**GM2**	**D**
Thickness (mm)	7.84 ± 0.03	7.99 ± 0.03	8.95 ± 0.05
Diameter (mm)	19.95 ± 0.02	20.06 ± 0.01	20.05 ± 0.02
Hardness (*N*)	40.6	44.5	45.3
Friability (%)	0.78	0.93	0.97
Weight variation (g)	2.21 ± 0.05	2.2 ± 0.07	2.94 ± 0.02
Effervescence time (sec)	90.6 ± 2	108.6 ± 2.19	117 ± 2
pH of solution	5.18 ± 0.05	5.32 ± 0.08	5.11 ± 0.02
Water content (g)	0.034	0.028	0.046
CO_2 content (mg)	227	236	214
Content uniformity (mg)	47.82 ± 0.16	48.68 ± 0.10	47.45 ± 0.29

DISCUSSION

In comparison to other iron salts, anhydrous ferrous sulfate provides more elemental iron (36 %) and has more water solubility. For these reasons, ferrous sulfate was selected to be used in the formulation of effervescent tablets (WHO, 2019).

Approximately 5–10 % of dietary iron is absorbed. Although the absorption percentage increases by up to 30 % in iron deficiency states, unabsorbed dietary iron lead to gastrointestinal disturbances. Ascorbic acid consumption is the most efficient enhancer of iron absorption (Abbaspour *et al.,* 2014). Therefore, the main aim of this study was the development of effervescent tablets containing these two ingredients to reduce the side effects of iron supplementation. The ratio of effervescent components in the formulation should result in a clear solution at acceptable effervescent time and pH <6. The amount of anhydrous citric acid was calculated slightly more than this stoichiometric ratio to enhance effervescent solution taste and reduce the rate of sodium ascorbate formation. In comparison, acid: base ratios that show low solubility and precipitation were not selected for the formulation.

The mean diameter of particles is increased by wet granulation due to the adhesion of smaller particles and the formation of larger particles. According to the curves of Figure 4, the mean particle size for the granule mixture prepared by the wet granulation method-2 is larger than the other two methods because more ingredients of the formulation were granulated in this method.

As the results are shown in the Table 2, the angle of repose is decreased with increasing granulated content of mixtures due to the increase in particle size and shape-changing into the sphere (Agrawal and Naveen, 2011). The Hausner ratio and the compressibility index are also reduced due to less significant inter particulate

interactions and closer bulk and tapped densities in mixtures containing higher granulated content, thus indicating improved powder flow.

Wet granulation improves tablet hardness due to the internal porosity of granules and plastic deformation (Agrawal and Naveen, 2011). In the direct compression method, the dry form of the PVP K-30 binder was used, and the powder mixture was pressed with a higher compression force to achieve the desired tablet hardness. The formulation was also granulated using a PVP K-30 binder solution in the wet granulation methods. Using an appropriate binder percentage in the formulation can eliminate capping problem during tablet processing. With the increase of PVP percentage, an increase in hardness and effervescence time was observed (Yanze *et al.,* 2000).

The thickness of the tablets must be within the range of 7.9 ± 0.1 mm so that the results are acceptable according to the pharmacopeia criteria (USP31–NF26, 2008). According to the EP, in the tablets weighing more than 250 mg, out of 20 tablets, only two tablets can exceed ± 5 % of the average weight, that the results are acceptable.

A pH of less than six is required to increase the absorption of effervescent solutions that the pH of the developed formulation is between 5.09 and 5.4 which is lower than six. Similar results of pH measurements in different samples of one formulation show that the granule mixtures were uniform (Yanze *et al.,* 2000). The effervescence time must be less than 5 minutes for the produced effervescent tablets that the results follow this requirement (WHO, 2019).

As each tablet contains 500 mg of sodium bicarbonate, so this amount will react with the anhydrous citric acid in the presence of water to produce a maximum of 262 mg of CO_2 per tablet which is comparable with the results. Lower levels of CO_2 content indicate that the moisture absorbed by the hygroscopic ingredients existing in the formulation has initiated a small-scale effervescent reaction.

As shown in Table 3, the friability of the tablets is acceptable. It was also observed that in large dimension tablets such as effervescent tablets with increasing hardness, the fragility also increases.

Anhydrous ingredients are extremely hygroscopic since they try to absorb moisture and return to their stable crystalline form. As a result, the possibility of initiating effervescent reaction and instability in effervescent tablets is high. The use of lactose anhydrous instead of sucrose in the GM2 provided better results because lactose anhydrous is less hygroscopic compared to powder sucrose. Also, sucrose crystalline is less

hygroscopic compared to powder sucrose, so crystalline form was used in the direct compression method. The produced tablets by the wet granulation method contain lower water content due to receiving heat during the drying process.

Since the amount of active ingredient ($FeSO_4$) can be variable in the range of 47.16 to 48.78 mg, the content uniformity of prepared effervescent tablets by all three methods was in the limits of USP acceptance criteria.

It was preferred to use orange or lemon flavors to mask the metallic taste of iron. However, when the amount of ferrous sulfate is calculated at the maximum recommended daily dose, full masking of metallic taste will become a challengeable problem.

CONCLUSION

This study attempted to formulate and produce effervescent tablets containing ferrous sulfate and ascorbic acid combination using direct compression and wet granulation methods. The results of this study show that both methods are applicable, but wet granulation is a more suitable method to produce ferrous sulfate effervescent tablets. This method is performed by adding a granulator solution to the powder mixture to obtain a wet mass. In this study, the evaluation results are in accordance with the pharmacopoeia criteria.

The produced effervescent tablets by the wet granulation method were more compact and uniform in content. They did not have any of the processing problems, but generally, effervescent tablets should be pressed using PTFE coated punches at a maximum of 30 % RH to overcome their sticking problem.

The developed formulation is acceptable for all physicochemical properties, including effervescent time less than 5 minutes, pH <6, friability below 1 %, water content under 0.5 %, low weight variation, and proper content uniformity. The metallic taste of ferrous sulfate was also masked by adding lemon flavor as much as possible.

These tablets are very useful in iron deficiency conditions because their ascorbic acid content can increase iron absorption and reduce iron supplementation related gastrointestinal side effects.

REFERENCES

Abbaspour N, Hurrell R, Kelishadi R (2014). Review on iron and its importance for human health. *J Res Med Sci.* **19**(2): 164-174.

Agrawal R, Naveen Y (2011). Pharmaceutical processing–A review on wet granulation technology. *International journal of pharmaceutical frontier research.* **1**(1): 65-83.

Allen LV, Popovich NG, Ansel HC (2011). Ansel's pharmaceutical dosage forms and drug delivery systems (9th ed.). Philadelphia: Wolters Kluwer Health/Lippincott Williams & Wilkins.

Altomare E, Vendemiale G, Benvenuti C, Andreatta P (1997). Bioavailability of a new effervescent tablet of ibuprofen in healthy volunteers. *Eur J Clin Pharmacol.* **52**(6): 505-506.

Ashish P, Mishra P, Main P, Harsoliya MA, Agrawal S (2011). A review on-recent advancement in the development of rapid disintegrating tablet. *Indian journal of life sciences and pharma research.* **1**(1): 7-16.

Aslani A, Fattahi F (2013). Formulation, characterization and physicochemical evaluation of potassium citrate effervescent tablets. *Adv Pharm Bull.* **3**(1): 217-225.

Aslani A, Sharifian T (2014). Formulation, characterization and physicochemical evaluation of amoxicillin effervescent tablets. *Advanced biomedical research.* **3**: 209.

Aulton ME, Taylor KM (2013). Aulton's Pharmaceutics: The Design and Manufacture of Medicines (4th ed.). London: Churchill Livingstone.

Boccio JR, Iyengar V (2003). Iron deficiency: causes, consequences, and strategies to overcome this nutritional problem. *Biol Trace Elem Res.* **94**(1): 1-32.

Callahan J, Cleary G, Elefant M, Kaplan G, Kensler T, Nash R (1982). Equilibrium moisture content of pharmaceutical excipients. *Drug Development and Industrial Pharmacy.* **8**(3): 355-369.

Conway BR (2008). Solid Dosage Forms. In S. C. Gad (Ed.), Pharmaceutical Manufacturing Handbook: Production and Processes (pp. 233-265). New York: John Wiley & Sons Inc.

Hadisoewignyo L, Soegianto L, Ervina M, Wijaya I, Santoso S, Tania N, Tjandrawinata RR (2016). Formulation Development and Optimization of Tablet Containing Combination of Salam (Syzygium Polyanthum) and Sambiloto (Andrographis paniculata) Ethanolic Extracts. *International Journal of Pharmacy and Pharmaceutical Sciences.* **8**(3): 267-273.

Heinrich H (1974). Iron preparation and process for its manufacture. In: Google Patents.

Japanese Pharmacopoeia (2002). Ferrous Sulfate / Official Monographs for Part I. In *Japanese Pharmacopoeia* (14th ed., pp. 474).

Kasperek R, Zimmer L, Zun M, Dwornicka D, Wojciechowska K, Poleszak E (2016). The application of povidone in the preparation of modified release tablets. *Current Issues in Pharmacy and Medical Sciences.* **29**(2): 71-78.

Lachman L, Lieberman HA, Kanig JL (1986). The theory and practice of industrial pharmacy (3rd ed.). Philadelphia: Lea & Febiger.

Moghimipour E, Akhgari A, Ghasemian Z (2010). Formulation of glucosamine effervescent granules.

Mohrle R (1989). Effervescent tablet. In *Pharmaceutical dosage form: tablets,* (2nd ed., Vol. 1, pp. 285-292)Liberman L, Lachman L, Schwartz JB (Eds.), New York: Marcel Dekker.

Ozyurt C, Evcin A(1994). P269 studies on formulations of foaming effervescent vaginal tablets. *European Journal of Pharmaceutical Sciences.* **2**(1-2): 186.

Ozyurt C, Evcin A (1994). Studies on Formulations of Effervescent Vaginal Suppositories. *Ankara Universitesi Eczacılık Fakultesi Dergisi.* **23**(1): 21-36.

Palanisamy P, Abhishekh R, Yogan and Kumar D (2011). Formulation and evaluation of effervescent tablets of aceclofenac. *Int Res J Pharm.* **2**(12): 185-190.

Patel H, Chauhan P (2012). Formulation and Evaluation of Effervescent Tablet of Paracetamol and Ibuprofen. *International Journal for Pharmaceutical Research Scholars.* **1**(2): 509-520.

Remington JP (2011). Remington: The Science and Practice of Pharmacy. In (pp. 895-896): Pharmaceutical Press.

Rowe RC, Sheskey PJ, Quinn ME (2009). Handbook of Pharmaceutical Excipients (6th ed.). London: Pharmaceutical Press.

Saleh S, Boymond C, Stamm A (1988). Preparation of direct compressible effervescent components: spray-dried sodium bicarbonate. *International journal of pharmaceutics.* **45**(1-2): 19-26.

Swarbrick J, Boylan J (2002). *Encyclopedia of pharmaceutical technology*. New York: Marcel Dekker.

Tolkien Z, Stecher L, Mander AP, Pereira DI, Powell JJ. (2015). Ferrous sulfate supplementation causes significant gastrointestinal side-effects in adults: a systematic review and meta-analysis. *PloS one.* **10**(2): e0117383.

USP26 (2002). The United States Pharmacopeia USP 26: The National Formulary NF 21. Rockville, MD: United States Pharmacopeial Convention.

USP31–NF26 (2008). Rockville MD USA: United States Pharmacopeial Convention.

WHO (2019). The International pharmacopoeia: Monographs: Dosage forms: General monographs: Tablets (9th ed.): Geneva: World Health Organization.

WHO (2019). The International pharmacopoeia: Monographs: Pharmaceutical substances: Ferrous sulfate. 9th. Retrieved from https://apps.who.int/phint/en/p/docf/anchor,finding-information.html

Yanze F, Duru C, Jacob M (2000). A process to produce effervescent tablets: fluidized bed dryer melt granulation. *Drug Development and Industrial Pharmacy*. **26**(11): 1167-1176.

Research Article EMUJPharmSci ISSN 2651-3587 https://dergipark.org.tr/emujpharmsci

EMU Journal of Pharmaceutical Sciences

EMUJPharmSci

Study of *in vitro* immunomodulatory effect and quantitative evaluation of main phytoconstituents in Indian *Drosera* species

Raju Asirvatham*, Aparna Ann Mathew, Salwa Abdul Salam

St. Joseph's College of Pharmacy, Department of Pharmacology, Kerala, India.

Abstract

The present study compared the total flavonoid content in ethanol and aqueous extracts of Indian Drosera and their *in vitro* immunomodulatory activities. None of the medicinally important compounds from this species has been quantified and compared previously. HPTLC method was used to quantify plumbagin and quercetin content in the ethanol extracts of three Indian *Drosera* species.

The *in-vitro* immunomodulatory activities of both ethanol and aqueous extracts were evaluated by the inhibition of heat and hypotonic induced hemolysis, nitroblue tetrazolium (NBT) assay and by inhibition of TNF-α release in DAL cell lines.

Ethanol extract of *D. burmannii* showed significant inhibition of heat and hypotonic induced hemolysis when compared with diclofenac. In NBT reduction test, ethanol extract of *D. burmannii* showed significantly higher reduction than *D. indica* and *D. peltata*. Inhibition of TNF-α release was significantly enhanced by 400 µg/mL of *D. burmannii.* Higher concentration of flavonoid was found in the ethanol extract of *D. burmannii*. Flavonoid concentration was the least in aqueous extract of *D. indica.* The calibration curve of plumbagin and quercetin were found to be linear (200 -1000 ng/spot). Correlation coefficient of r = 0.9994 ± 8.62 and r= 0.99068 ± 13.63 was detected for plumbagin and quercetin, respectively. This is indicative of good linearity between concentration and peak area.

The identity of the plumbagin and quercetin band in the sample extracts was confirmed by comparing the UV absorption spectrum of the sample to that of the reference standard plumbagin and quercetin, using the Camag TLC scanner. Higher concentrations of plumbagin and quercetin were found in the ethanol extract of *D. burmannii.* The proposed HPTLC method provided good resolution and accuracy, and can be practiced for the rapid determination of plumbagin and quercetin in the herbal drugs. Such an approach is effective for routine quality control analysis and quantification of plumbagin. The pharmacological actions of the species investiagted are due to its chief chemical constituents.

Keywords

High-performance thin liquid chromatography, immunomodulatory, Indian *Drosera*, plumbagin, quercetin, quantification.

Article History

Submitted: 18 February 2020 Accepted: 01 March 2020 Published Online: March 2020

Article Info

***Corresponding author:** Raju Asirvatham **e-mail:** rajuasirvatham@gmail.com

Research Article:

Volume: 3 Issue: 1 March 2020 Pages: 50-63

INTRODUCTION

Drosera plants belonging to family Droseraceae are commonly known as sundew plants. *Drosera* consists of approximately 170 species (Jayaram and Prasad 2006). Three species of *Drosera* are found in India, viz., *D. burmannii* Vahl, *D. indica* L., and *D. peltata* J.E.Sm (Santapau and Henry 1976). The genus *Drosera* contains naphthoquinones such as plumbagin,7-methyljuglone and flavonoids with various important pharmacological activities. Plumbagin is used for curing bronchial infection, whooping cough, hyperglycaemia, hypolipidaemia, tuberculosis, spasms, cancer, fertility problems, arteriosclerosis, phthisis, asthma; leprosy, leishmaniasis and malaria. Moreover, it acts as immunomodulator, cosmetics, aphrodisiac, chitin synthetase inhibitor, insecticide, antifeedant and abortifacient. It enhances phagocytic activity of human granulocytes *in-vitro* and inhibits the development of insect and parasitic nematodes. 7- Methyljuglone is shown to be inhibitory to several insects and is highly toxic to fungal pathogens (Raju *et al.,* 2012, Yu He *et al.,* 2012). Literature review fails to claim the study of immunomodulatory effects (*in-vitro*) of these Indian *Drosera* species. Therefore, in this study it was aimed to evaluate the immunomodulatory potency of the three Indian *Drosera* species and quantify the variation in the amount of plumbagin and quercetin among different species. High Performance Thin Layer Chromatography (HPTLC) is an efficient tool for phytochemical evaluation of herbal drugs. However, no HPTLC method has been developed for the quantification of plumbagin and quercetin in the ethanol extracts of *D. burmannii*, *D. indica* and *D. peltata*. The HPTLC method proposed in the study is simple, precise and sensitive.

MATERIALS AND METHODS

Plant material

The whole plants of *D. burmannii* and *D. indica* L. were collected during December 2010, from the forests of Savanadurga, Karnataka, India. The plant material was identified and authenticated by Dr. S.N. Yoganarasimhan, a taxonomist and research coordinator at M. S. Ramaiah College of Pharmacy, Bangalore, Karnataka, India. The whole plant of *D. peltata* was collected from the hills of Munnar, Kerala, India. It was identified and authenticated by Dr. Madava Chetty, Asst. Professor, Department of Botany, Sri Venkateshwara University, Tirupathi. All the voucher specimens have been

deposited at the Department of Pharmacognosy, Shri Rawatpura Sarkar Institute of Pharmacy, Datia, (M.P) (Herbarium No :SRIP/COGNOSY/2011-04,05&06). Plant materials were washed, shade dried, powdered, passed through sieve no. 60 and stored in air tight containers for further experiments.

Preparation of the extracts

Shade dried, powdered samples were subjected to successive solvent extraction with petroleum ether (60-80 °C), followed by chloroform and ethanol (90 % *v/v*) in a Soxhlet extractor. The extract was concentrated in a rotary flash evaporator at a temperature not exceeding 50 ºC. The ethanol extracts were suspended in distilled water for experimental purpose.

Determination of flavonoid content

The content of flavonoids, expressed as flavones and flavonols, was quantified from the ethanol and aqueous extracts of *D. burmannii* Vahl, *D. indica* L., and *D. peltata* J.E.Sm by colorimetric method using aluminum chloride ($AlCl_3$) (Bag GC *et al.,* 2015).

Preparation of calibration curve

100 µg/mL quercetin solution was prepared in methanol as stock solution and then diluted to get final concentrations of 2, 5, 10, 15 and 20 µg/mL. To 0.5 mL of these diluted solution, 1.5 mL of methanol, 0.1 mL 1 M of potassium acetate (CH_3COOK), 2.8 mL of H_2O and 0.1 mL of $AlCl_3$ (10% in distilled water) were added. The final reaction mixtures were thoroughly mixed and kept for 30 minutes at 32ºC. After incubation, the absorbance was read at 415 nm using a UV spectrophotometer. 0.1 mL of distilled water instead of $AlCl_3$ was used as blank. Standard calibration curve for quercetin was graphed by various concentrations at X axis and absorbance at Y axis.

Sample preparation

10 mg of each ethanol and aqueous extracts of *D. burmannii*, *D. indica* and *D. peltata* were dissolved in 2.5 mL of methanol using vortex agitator. The extracts were filtered to remove the solid residue. The final volume was adjusted to 5 mL with methanol.

Procedure

An aliquot of 0.5 mL of each extract (concentration from 1 to 10 mg/mL) was added to1.5 mL of methanol, 0.1 mL 1 M of CH_3COOK, 2.8 mL of H_2O and 0.1 mL of 10% $AlCl_3$. Later, the absorbance was read at 415 nm. Total flavonoid content in the extracts was computed from the quercetin standard graph and the quantity was expressed in mg/g quercetin equivalent (QE) or % w/w of the extractives.

Study of preliminary immunomodulatory properties

The preliminary immunomodulatory properties of ethanol extracts of all Indian species were evaluated by the procedure described by Suresh Kumar *et al*. (2017).

Heat induced hemolysis

The assay mixture contains 1 mL phosphate buffer (pH 7.4, 0.15 M), 2 mL hyposaline (0.36 %), 0.5 mL human red blood cell (HRBC) suspension (10 % v/v) with 0.5 mL of all extracts and standard drug diclofenac sodium (200 µg/mL) at various concentrations (50, 100, 200, 400, 800, 1000 µg/mL). Distilled water instead of hyposaline that produces 100 % hemolysis was used as control. The assay was carried out in triplicate manner. The mixtures were incubated at 40 ºC for 30 minutes and centrifuged. The hemoglobin content in the suspension was estimated using spectrophotometer at 560 nm.

The percentage of hemolysis was calculated as follows:

% Hemolysis = (Optical density of test sample / Optical density of control) X 100

The percentage of HRBC membrane stabilization can be calculated as follows:

% Protection = 100 – [(Optical density of test sample / Optical density of control) X 100].

Hypotonic induced hemolysis

Samples of the extracts were dissolved in hypotonic solution (0.2% sodium chloride). The hypotonic solutions (5 mL) of graded doses of the extracts (50, 100, 200, 400, 600, 800 and 1000 µg/mL) were taken in triplicate manner (per dose) in centrifuge tubes. Control tubes contained 5 mL of the vehicle (distilled water) and standard tubes included 5 mL of 200 µg/mL diclofenac sodium. Erythrocyte suspension (0.1 mL) was added to each of the tubes and mixed gently. The mixtures were incubated for one hour at room temperature (30°C) and afterwards, centrifuged for 3 minutes at 3000 rpm. Absorbance of the hemoglobin content in the supernatant was estimated at 540 nm using spectrophotometer. The hemolysis percentage was calculated by assuming the hemolysis produced in the presence of distilled water as 100%. The percentage of the inhibition of hemolysis by the extracts was calculated using the formula:

% Hemolysis = (Optical density of test sample / Optical density of control) X 100

The percentage of HRBC membrane stabilization was calculated as follows:

% Protection = 100 – [(Optical density of test sample / Optical density of control) X 100]

Nitroblue Tetrazolium (NBT) assay on haemocytes

The reduction of NBT to insoluble blue formazan was used as an indicative for superoxide generation, although it is not entirely specific for O_2^-. A measured

volume of haemocytes were loaded, in triplicate, in 96 well microtiter plate (Sigma M-0156) and incubated with different concentration of extracts under humid conditions for 30 minutes at room temperature for the adherence of the hemocytes. The supernatants were removed and 0.3% NBT and absolute methanol were added. The formazan deposits were solubilized in 120 mL 2 M KOH and 140 mL dimethyl sülfoksit (DMSO). After homogenization of the contents in the wells, the absorbance was read at 620 nm in spectrophotometer.

TNF-α inhibition assay

Inhibition of TNF-α release in lipopolysaccharide (LPS) stimulated DAL cells was assayed using a slight modification of procedure suggested by Weiss *et al.* (1982). Different concentrations of extracts and LPS were added to induce inflammation in measured volume of cell line and kept aside for three hours. Then, the cells ($1x10^6$ cells/mL) were transferred to a 96 well microplate and incubated at 37 °C for 18 hours. After an overnight incubation, the plate was centrifuged (1800 g, 5 minutes, 16 °C), the supernatant was collected and TNF-α was quantified by the cytokine-specific sandwich quantitative enzyme-linked immune-sorbent assay (ELISA), according to the manufacturer's instructions. The inhibition of TNF-α release by LPS-stimulated DAL cells was calculated by the ratio between the TNF-α amount (pg/mL) secreted by treated cells and nontreated cells that were stimulated with LPS. TNF-α inhibition was reported as percentage values: [1 − (cytokine secretion of treated cells/cytokine secretion of cells cultivated with solvent control) x 100].

HPTLC study

Instruments and chemicals

CamagLinomat V automatic sample spotter, Camag (Muttenz, Switzerland), Camag TLC Scanner III linked to winCATS software (Camag), Camag glass twin trough chamber (10 x 10 cm) were used. Silica gel $60F_{254}$ (E. Merck, India) coated aluminum sheet plates were employed. Toluene and glacial acetic acid were used as mobile phase. Standard plumbagin and quercetin was obtained from Sigma Aldrich.

Preparation of standard solution

Standards of plumbagin and quercetin were prepared by dissolving 1 mg of standard in 5 mL of methanol. The solutions were sonicated for 10 minutes and the volume was adjusted to 10 mL with methanol, to obtain a working standard solution of 100 µg/mL concentration.

Preparation of sample solution

Stock solutions of the samples were prepared by transferring 1 mg of accurately weighed ethanol extracts of *D. peltata*, *D. burmanii* and *D. indica* in 10 mL

volumetric flask and 5 mL of methanol was added. The volumetric flask was sonicated for 15 minutes at room temperature. The flask content was filtered through Whatman filter paper No. 1 (Merck, Mumbai, India). The filtrate was collected and the volume was adjusted to 10 mL with methanol.

Procedure

HPTLC experiments were carried out by following standard procedures (Madhavan *et al.,* 2008; Wagner *et al.,* 1984). The working standard solutions of plumbagin and quercetin (100 ng in 1 µl) were spotted (2 µl) to get different concentrations ranging from 200 – 1000 ng/spot, using a micro-syringe. The working standard solutions were spotted as sharp band of 6 mm width using Camag 100 µl sample syringe on precoated silica gel aluminum plate $60F_{254}$ (10cm x 10cm) using a CamagLinomat V automatic sample applicator. The bands were applied at a distance of 10 mm from the bottom edge of the plate. The distance between the two bands was 11.4 mm. Total 8 spots were applied. First 5 spots were standard plumbagin and quercetin (concentrations of 200, 400, 600, 800 and 1000 ng/spot) and the next 3 spots were 5 µl of sample solution of ethanol extracts of *D. peltata*, *D. burmanii* and *D. indica*. The plates were developed in the solvent system comprising of toluene:glacial acetic acid (55:1) in a Camag glass twin trough chamber at 25 ± 2 °C, up to a distance of 70 mm. After the development, the plates were dried by a dryer for 5 minutes. Densitometric scanning was performed on a Camag TLC scanner 3 in the reflectance absorbance mode at 254 nm for all measurements, operated by CATS 3 software.

Statistical analysis

Data were statistically analyzed by Student's t-test and $p<0.01$ was considered to be significant. For efficacy assessments, one way ANOVA and Dunnet's t test were used. All the tests were performed in triplicate.

RESULTS

The effects of ethanol extracts of *D. burmannii, D. indica* and *D. peltata* on the inhibition of hemolysis under two different conditions (hypotonic solution and heat) were expressed in Table 1. Ethanol extract of *D. burmannii* showed significantly ($p< 0.001$) higher inhibition of hemolysis than *D. peltata*. *D. indica* revealed the least inhibition ($p< 0.01$).

Table 1: Inhibition of hypotonic solution and heat induced haemolysis of erythrocyte membrane by Indian *Drosera* species ethanol extracts.

	Sample concentration (Ethanol extracts µg/mL)	% Inhibition of haemolysis*	
		Hypotonic solution	Heat induced
D. burmannii	50	11.6±1.4	15.6±4.2
	100	23.5±3.4	25.6±1.2
	200	42.6±3.8	46.5±3.4
	400	68.4±2.9	69.2±1.6
	800	88.4±1.3	87.8±1.9
	1000	91.5±2.2	93.6±2.4
D. indica	50	1.1±2.2	6.4±3.6
	100	8.5±3.1	12.7±1.0
	200	16.4±1.3	21.6±1.9
	400	23.5±1.1	26.5±4.2
	800	46.2±4.3	52.6±2.4
	1000	52.6±2.3	59.7±1.5
D. peltata	50	3.1±1.6	5.3±2.2
	100	10.5±2.2	11.6±1.3
	200	22.7±1.1	37.4±2.4
	400	49.4±3.1	51.6±3.1
	800	70.8±1.3	76.2±1.3
	1000	82.5±2.1	86.7±2.1
Diclofenac	200	90.4±1.0	88.8±2.4

*mean±SD (n=3)

The results of ethanol extracts of *D. burmannii, D. indica* and *D. peltata* with respect to NBT reduction were shown in Table 2. All of the ethanol extracts increased the NBT reduction concentration dependently. The highest increase in the reduction was detected in extracts of *D. burmanii* followed by *D. peltate* and *D. indica*, respectively.

Table 2: Effect of Indian *Drosera* species extracts on NBT reduction test.

Plant name	Sample concentration (µg/mL)	Mean (%) ±SD
D.burmanni	50	11.6±1.4
	100	23.5±3.4
	200	42.6±3.8
	400	68.4±2.9
	800	88.4±1.3
	1000	91.5±2.2
D.indica	50	1.1±2.2
	100	8.5±3.1
	200	16.4±1.3
	400	23.5±1.1
	800	46.2±4.3
	1000	52.6±2.3
D.peltata	50	3.1±1.6
	100	10.5±2.2
	200	22.7±1.1
	400	49.4±3.1
	800	70.8±1.3
	1000	82.5±2.1

Effect of ethanol extracts of *D. burmannii, D. indica* and *D. peltata* on the inhibition of TNF-α release by LPS-stimulated DAL cells were shown in Table 3. All the extracts inhibited the secretion of TNF-α. The higher the concentration was, the more the inhibition was observed. Ethanol extracts of *D. burmannii* was detected to have the highest percentage of inhibition; followed respectively *by D. peltata and D. indica.*

Total flavonoid content present in all the extracts was estimated by using $AlCl_3$. The amount of flavonoids present in each extracts was expressed as mg/g (QE) and shown in Table 4.

Table 3: Inhibition of TNF-α release on LPS-stimulated DAL cells.

	Concentration of extracts (µg/mL)	Inhibition of TNF-α (% ± SD)
D.burmannii	100	12.4±2.1
	200	59.6±1.4
	400	92.6±2.1
D. indica	100	9.5±2.5
	200	42.3±1.3
	400	72.3±1.8
D. peltata	100	10.3±1.4
	200	48.8±1.8
	400	90.7±2.7
Control	-	12.6±2.1
Dexamethasone	(0.1 µM)	87.5±1.3

Table 4: The total flavonoid quantity in *Drosera* species.

Concentration of extracts (µg/mL)	Total flavonoid content in mg/g (QE)*, **					
	EEDB***	AEDB***	EEDI***	AEDI***	EEDP***	AEDP***
100	0.235± 0.004	0.111± 0.003	-0.04± 0.009	-0.039± 0.02	0.242± 0.002	0.096± 0.009
250	0.448± 0.021	0.309± 0.109	0.016± 0.004	-0.03± 0.02	0.465± 0.002	0.224± 0.013
500	0.633± 0.021	0.459± 0.002	0.111± 0.004	0.024± 0.02	0.598± 0.02	0.354± 0.022
750	0.986± 0.078	0.606± 0.003	0.182± 0.064	0.143± 0.011	0.896± 0.006	0.484± 0.009
1000	1.204± 0.021	0.672± 0.028	0.402± 0.014	0.221± 0.007	1.051± 0.024	0.607± 0.012

*QE=quercetin equivalent;
**mean±SD (n=3)
***EEDB- Ethanol extract of *D. burmannii,* AEDB- Aqueous extract of *D. burmannii* ,EEDP - Ethanol extract of *D. peltata,* AEDP- Aqueous extract of *D. peltata,* EEDI- Ethanol extract of *D. indica*, AEDI- Aqueous extract of *D. indica.*

The total flavonoid content in three plants was presented as mg/g of Quercetin equivalent (QE) ± SD (n = 3). Both ethanol and aqueous extracts of *D. burmannii*, *D. indica* and *D. peltata* were tested at 1000, 750, 500, 250 and 100 µg/mL and the positive control (Quercetin) at 10, 7.5, 5.0, 2.5 and 1 µg/mL. Higher concentrations of flavonoid were found in ethanol extract of *D. burmanii* whereas the concentration was the least in aqueous extract of *D. indica*. The order of total flavonoid content with respect to plant was *D. burmannii>D. peltata>D.indica* for the concentrations

500 µg/mL and over. For 100 and 250 µg/mL, the amount of flavonoid was only slightly higher in *D. peltata* than *D. burmanii*. Ethanol extracts of all species contained significantly higher concentration of flavonoids than aqueous extracts.

The flavonoid contents were estimated from the standard calibration curve of quercetin. 10, 7.5, 5.0, 2.5 and 1 µg/mL concentration of quercetin were plotted at X axis and the corresponding absorbances were plotted at Y axis, which was represented in Figure 1.

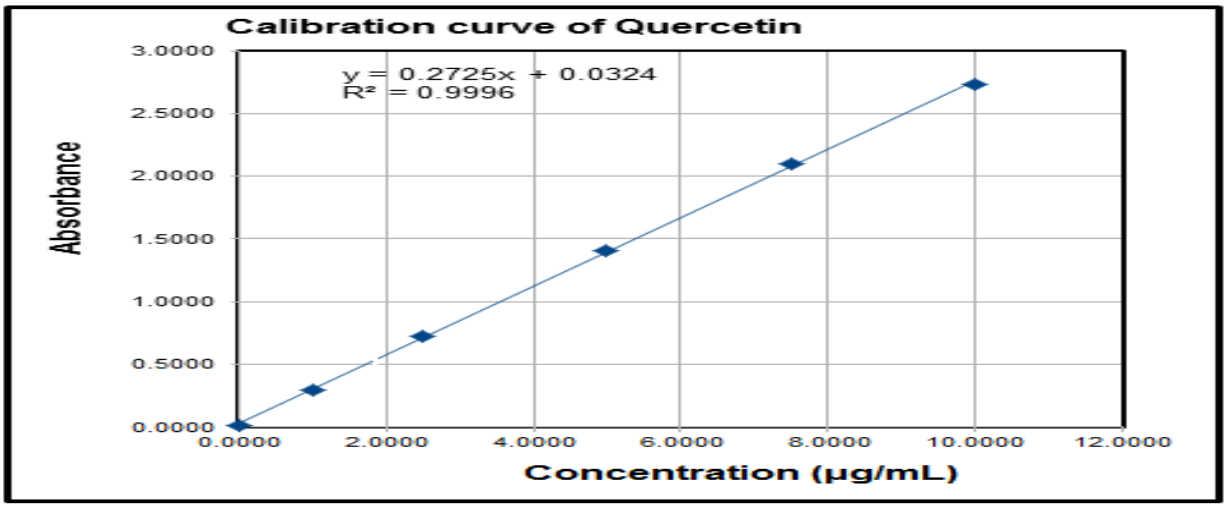

Figure 1: Calibration curve of quercetin for determination of total flavonoid content.

Plumbagin and quercetin from the sample solution and standard spots were well separated from other compounds in HPTLC condition. Their peaks displayed excellent peak resolutions as shown in Figure 2 and 3. The TLC plate was visualized under UV light at 254 nm. The HPTLC photographed chromplate is shown in Figure 4 and 5. In total flavonoid content determination, aluminum chloride reacts with carbonyl group at C4 and hydroxyl at C3 (flavonols) and C5 in flavonols and flavones to form acid stable as well as unstable complexes. Chromatographic analysis that was performed using ethanol extracts of three plants, on pre-coated silica gel HPTLC plates $60F_{254}$, using solvent system comprising of Toluene:Glacial Acetic Acid (55:1) as mobile phase gives good separation of plumbagin at R_f =0.83 to 0.88. Similarly, using a solvent system, comprising of toluene:ethyl acetate: formic acid:methanol (3:6:1.6:0.4 *v/v/v/v*) as mobile phase gives good separation of quercetin at R_f =0.76 and 0.77. Detection and quantification of plumbagin and quercetin were done by densitometric scanning at λ = 254 nm.

The calibration curves (Figure 6 and 7) of plumbagin and quercetin were found to be linear (200 - 1000 ng/spot) and dependent

on the concentration against area. The equation of best fitting line was Y = 2684 + 13.8 * X, r = 0.9994 sdv = 8.62 for plumbagin and Y = 1.309e + 004+12.1*X r= 0.99068 sdv= 13.63 for quercetin.

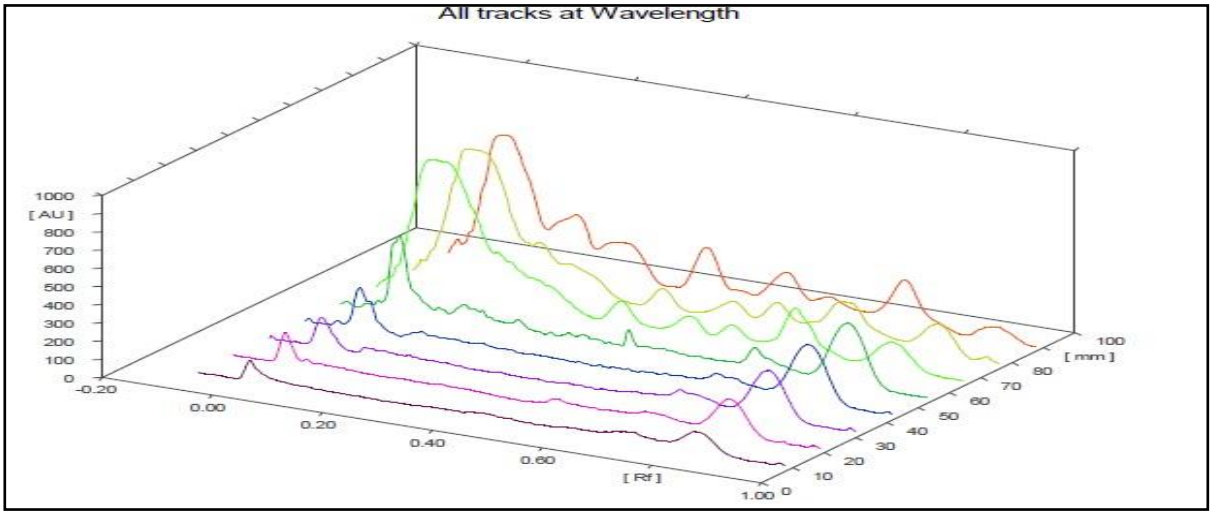

Figure 2: HPTLC chromatogram of plumbagin in all applied spots.

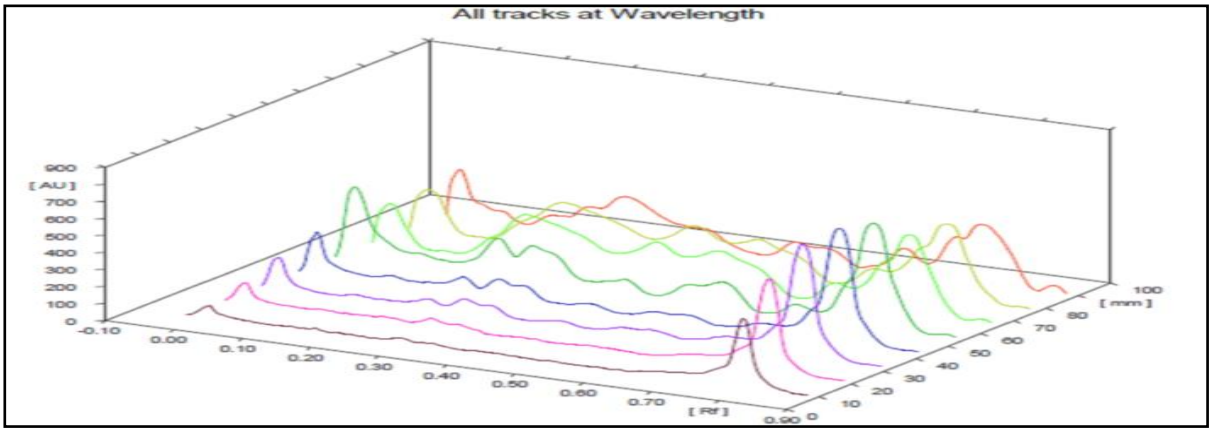

Figure 3: HPTLC chromatogram of quercetin in all applied spots.

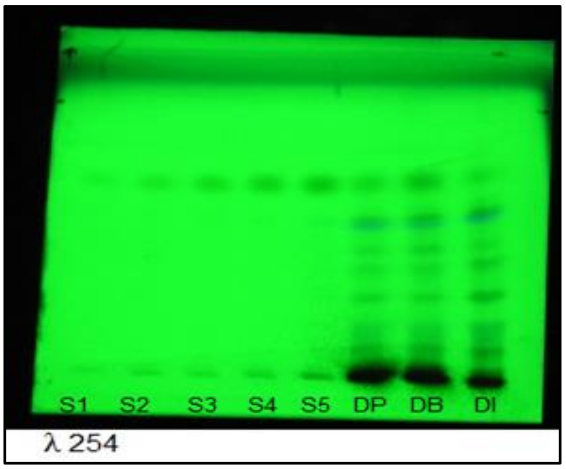

Figure 4: Photograph of plumpagin TLC plate at λ max 254.

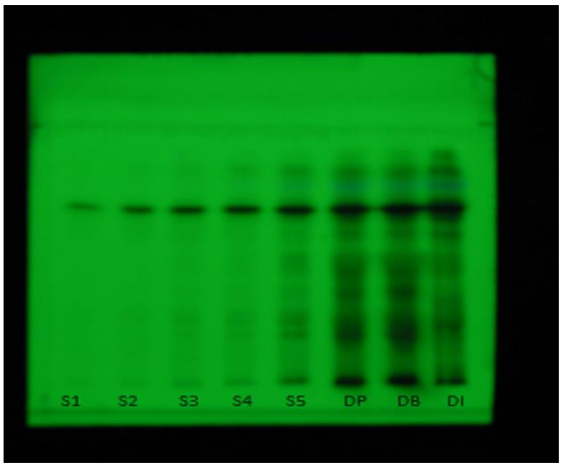

Figure 5: Photograph of quercetin TLC plate at λ max 254.

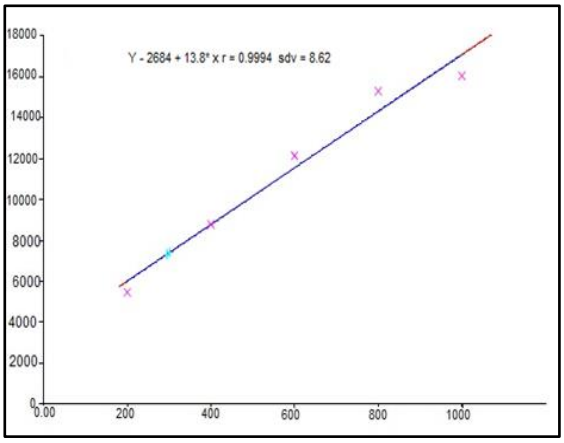

Figure 6: Quantification of plumbagin (Regression via area).

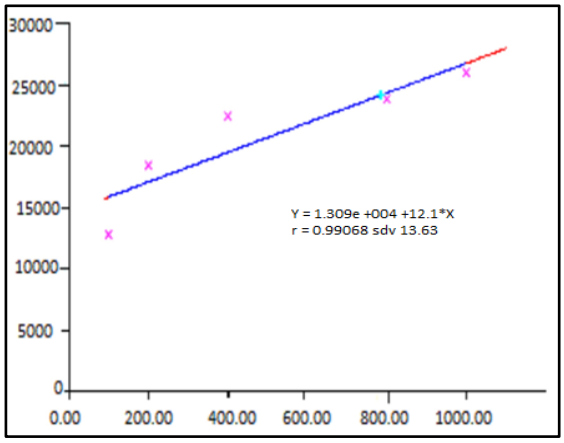

Figure 7: Quantification of quercetin (Regression via area).

From the HPTLC study, mg/g quantities of plumbagin and quercetin were calculated by regression via area, and the results are presented in Table 5. Ethanol extract of *D. burmannii* possesses higher concentration of plumbagin and quercetin when compared to *D. peltata* and *D. indica*. Plumbagin and quercetin concentration in *D. burmannii* was 1.572 and 0.6022 mg/g of extract, respectively. Similarly, plumbagin and quercetin concentration was 1.568 and 0.5884 mg/g in *D. peltata* and 0.9812 and 0.2471 mg/g for *D. indica*.

Table 5: Amount (mg) of quercetin and plumbagin found in per gram of ethanol extracts of Indian *Drosera* species.

Name of extracts	Amount of Quercetin/g of extract (mg/g)	Amount of Plumbagin /g of extract (mg/g)
EEDB*	1.572	0.6022
EEDP*	1.568	0.5884
EEDI*	0.9812	0.2471

*EEDB- Ethanol extract of *D. burmannii,* EEDP - Ethanol extract of *D. peltata,* EEDI- Ethanol extract of *D. indica*.

DISCUSSION

There is a link between cancer and inflammation because many researchers reported that naturally occurring anti-inflammatory or immunomodulatory plant metabolites have anticancer effect. The anticancer effect is due to the stimulation or inhibition of particular cellular inflammatory actions and the related molecular signaling pathways (Chien-Fu H *et al*., 2008). All the three plants investigated in the present study were reported to have anti-cancer effect on DAL and EAC cell line (Raju A *et al*., 2012). Immunomodulatory reaction was exhibited by stabilization of lysosomal membrane and thereby limiting the release from activated neutrophils of lysosomal constituents such as bactericidal enzymes and proteases. The release of lysosomal enzymes into the cytoplasm stimulates the inflammatory mediators such as oxygen radicals, prostaglandins and trigger the

inflammation (Balkwill *et al*., 2001). Many of NSAIDS stabilize lysosomal membrane and inhibit the inflammatory process by restricting the release of lysosomal enzymes. The results of the present study confirmed that all the ethanol extract of Indian *Drosera* species were able to stabilize RBC membrane against stress, like hypotonicity and heat. Inhibition of haemolysis indicates that all the extracts had the ability to prevent rupture or haemolysis of RBCs. Since there is a close similarity between RBC and lysosomal membrane, protection against hypotonic solution or heat induced lysis of RBC is often extrapolated to stabilization of lysosomal membranes. Therefore, inhibition of the haemolysis is used as a biochemical index of anti-inflammatory activity (Gandhidasan R *et al*., 1991). Researchers have already reported that, flavonoids, triterpenoids, and many other secondary plant metabolites can exhibit an algesic and anti-inflammatory effects as a result of their membrane stabilizing actions (Prasanna B *et al*., 2012). Similarly, ethanol extracts of Indian *Drosera* species exhibited statistically significant and concentration dependent membrane stabilization effect by inhibiting both hypotonicity and heat induced lysis of erythrocytes compared to the standard drug diclofenac sodium.

Furthermore, the ethanol extract of Indian *Drosera* species significantly increased the intracellular reduction of NBT dye to formazan (deep blue compound) by the neutrophils, confirming the increase in the intracellular killing property. The reduction was also determined to be concentration dependent.

As a part of host defense, upon inflammatory stimuli, such as LPS, macrophages trigger signals for the production of diverse inflammatory mediators, such as TNF-α and nitric-oxide. In tumor progression process, inhibition of TNF expression occur and is used to find out the possible mechanism of any anticancer drug. Researchers reported that a drug with anti-inflammatory or immunomodulatory property also inhibits TNF expression in host cell for defense purpose (Yamada Y *et al*., 1998). The present study results revealed that ethanol extracts of all Indian *Drosera* species possess concentration dependent inhibition on TNF-α release.

Our HPTLC results indicated that the whole plant extracts of Indian *Drosera* species contain various biologically active constituents such as plumbagin and quercetin. According to the quantity of constituents, each extract exhibited potency of inhibition and pharmacological action.

CONCLUSION

In conclusion, besides reports on various pharmacological actions of plumbagin and quercetin, no other literature is available for evaluation of their immunomodulatory activity although it has been used for the treatment of various diseases in Ayurveda, Sidha and traditional medicine. *Droserae* herbal drugs are remarkable for their anti-carcinogenic and anti-oxidant constituents such as plumbagin and quercetin. In the present research, plumbagin and quercetin content of the three Indian *Drosera* species were determined by a fast and sensitive HPTLC method. The method can be used for routine quality control analysis and for the quantitative determination of plumbagin and quercetin in other herbal and medicinal preparations.

ACKNOWLEDGMENTS

The authors gratefully acknowledge K M C H College of Pharmacy, Coimbatore, Tamil Nadu, for providing support and facilities for this research work. The authors also thank Dr. SN Yoganarasimhan for his guidance in the selection and collection of these plant materials.

REFERENCES

Bag GC, Grihanjali Devi P, Bhaigyabati TH (2015). Assessment of total flavonoid content and antioxidant activity of methanolic rhizome extract of three *Hedychium species* of manipur valley. *Int J Pharm Sci Rev Res* **30**(1): 154-159.

Balkwill, Mantovani A (2001). Inflammation and cancer: back to Virchow? *The Lancet* **357**(9255): 539–545.

Chien-Fu H, Shih-Shen L, Pao-Hsin L, Young SC, Yang CC (2008). The immunopharmaceutical effects and mechanisms of herb medicine. *Cellular and Molecular Immunology* **5**(1):23–31.

Gandhidasan R, Thamaraichelvan A (1991). Anti-inflammatory action of Lannea coromandelica by HRBC membrane stabilization. *Fitoterapia* **62**(1): 81–83.

Jayaram K, Prasad MNV (2006). *Droser aindica* L. and *D. burmanii* Vahl., medicinally important insectivorous plants in Andhra Pradesh –regional threats and conservation. *CurrSci* **91**:943-946.

Madhavan V, Basnett H, Kumar AC, Yoganarasimhan SN (2008). Fingerprinting of plumbagin in *Drosera burmannii* Vahl using high performance thin layer chromatography. *Indian J Pharm Sci* **70**:798-800.

Prasanna BG, Sameera RS, Ira TG, Weerasinghe AK, Mayuri GT, Ratnasooriya WD, Kamani HT (2012). Anti-inflammatory activity is a possible mechanism by which the polyherbal formulation comprised of *nigella sativa* (seeds), *Hemidesmusindicus* (Root), and *Smilax glabra* (Rhizome) mediates its antihepatocarcinogenic effects. *Evidence Based Complementary and Alternative Medicine*: 1-12.

Raju A , Christina AJM , Mayakrishnan A (2012). Antitumor potential of ethanol and aqueous extracts of *Drosera burmannii* Vahl against Dalton's ascitic lymphoma bearing mice. *J Pharm Res* **5**(3): 1418-1423.

Santapau H, Henry AN (1976). A Dictionary of the flowering plants in India. Publication and information Direcorate, pp.58, New Delhi, India.

Suresh Kumar Karri, Angappan Sheela (2017). Comparative in vitro Antidiabetic and Immunomodulatory evaluation of standardized five select medicinal herbs and spectral analysis of i L. (Nyctaginaceae). *PharmacognJ* **9**(3): 336-344.

Wagner H, Bladt S, Zgainski EM (1984). A Thin Layer Chromatography Atlas. In: Plant Drug Analysis – 2nd edn, pp. 276,Springer: Berlin, Germany.

Yamada Y, Webber EM, Kirillova I, Peschon JJ, Fausto N (1998). Analysis of liver regeneration in mice lacking type 1 or type 2 tumor necrosis factor receptor: requirement for type 1 but not type 2 receptor. *Hepatology* **28**(4I): 959–970.

Yu He, Zhimin He, Feng He, Haitong Wan (2012). Determination of quercetin, plumbagin and total flavonoids in *Droserapeltata* Smith var. glabrataY.Z.Ruan. *Pharmacogn Mag* **8**(32): 263–267.

Review EMUJPharmSci ISSN 2651-3587 https://dergipark.org.tr/emujpharmsci

EMU Journal of Pharmaceutical Sciences

EMUJPharmSci

A review of oxidants and antioxidants in biological systems

Imge Kunter*, Niloufar Zabib, Muberra Kosar

Eastern Mediterranean University, Faculty of Pharmacy, Famagusta, North Cyprus, Mersin 10 Turkey.

Abstract

Oxidants are any agent capable of removing electron from another molecule in a course of a redox reaction. When it comes to biological systems free-radicals, especially reactive oxygen species (ROS) and reactive nitrogen species (RNS) are involved in oxidation reactions. Both endogenous and exogenous factors can contribute to free-radical formation. Fortunately, an endogenous balance between free-radicals and antioxidant systems is present in the biological system. Despite the common belief that free-radicals are destructive agents, nowadays it has been proven that free-radicals such as ROS and RNS are greatly involved in signalling pathways and immune function. The destructive effect of antioxidants becomes significantly important only when this intrinsic balance is disturbed in favour of free-radicals, a condition known as oxidative stress. Over-production of free-radicals in oxidative stress can have deleterious effects on the biological systems in virtue of their interaction with important biological molecules such as proteins, lipids, and DNA. Favourably antioxidants are available to prevent the over-accumulation of free radicals and consequently their harmful effects by scavenging them. Various classification attributes have been suggested for antioxidants, amongst which, classification on the basis of their mechanism of action as primary and secondary antioxidant or their classification on the basis of their enzymatic activity as enzymatic and non-enzymatic antioxidants are the most famous ones. The objective of this review article is to provide the basic information required for the understanding of reactive oxygen species and their formation, antioxidants terminology, their classification and the mechanism by which the antioxidants are involved in counteracting harmful effect of oxidant in biological systems.

Keywords

Antioxidants, biological systems, oxidative stress, ROS, RNS.

Article History

Submitted: 22 December 2019 Accepted: 05 March 2020 Published Online: March 2020

Article Info

***Corresponding author:** ImgeKunter, **e-mail:** imge.kunter@emu.edu.tr

Research Article:

Volume: 3 Issue: 1 March 2020 Pages: 64-72

Free-radical terminology

Oxidant species are free-radicals with one or more unpaired electron present on the outer atomic or molecular orbital. Exogenous factors such as hyperoxia, smoking, exposure to ozone, and heavy metals or intrinsic factors like a respiratory chain reaction in mitochondria, oxidative reactions occurring in peroxisome for phagocytosis; can result in the formation of free-radicals (Phaniendra *et al.,* 2015). These newly synthesized free-radicals are highly unstable, and thus highly reactive to reach a stable configuration via either donating the unpaired electron or accepting an electron from other molecules. In biological systems, a free-radical lasts for a few milliseconds as it immediately reacts with the neighbouring molecules including but not limited to, proteins; nucleic acids and lipids, resulting in the conversion of non-radical molecules into free-radicals. This initial conversion is the start of an ongoing chain reaction producing millions of free-radicals (Tiwari, 2004). The chain reaction can be stopped by either two free-radicals cross-linkage pairing the unpaired electrons or antioxidant system interventions (Santo *et al.,* 2016).

Classification of oxidants in the biological systems

These oxidants are generally classified into two groups as reactive oxygen species (ROS) and reactive nitrogen species (RNS). In Table 1, a summary of the main endogenous antioxidants is provided (Dontha, 2016).

Table 1: Major endogenous oxidants present in the biological systems (Badarinath *et al.,* 2010).

Major endogenous oxidants	
Reactive oxygen species	**Formula**
Superoxide anion	O_2
Hydrogen peroxide	H_2O_2
Hydroxyl radical	OH
Hypochlorous acid	HOCl
Peroxyl radicals	ROO
Hydroperoxyl radical	HOO
Reactive nitrogen species	
Nitric oxide	NO
Peroxynitrite	$ONOO^-$

ROS generation within the biological systems

Because of intrinsic factors like, mitochondria involvement in respiratory chain reaction, endoplasmic reticulum role in CYP450 system, transition metal ion catalysed reaction and oxidative reactions occurring in peroxisome through phagocytosis the covalent bond can be broken leaving behind one electron from each pair, or in other words free-radical production. For instance, addition of one

electron to molecular oxygen, give rise to superoxide free-radical. As shown in Figure 1 this conversion is mediated by Nicotine Adenine Dinucleotide Phosphate (NAD(P)H) oxidase, Xanthine Oxidase (XAO/XO) or mitochondrial electron transport chain (ETC) (Gupta, 2015). Mitochondria are major sources of ROS; the main sites of superoxide radical production in the respiratory tract. Mitochondria are one of the major endogenous factors contributing to oxidative stress. Normally mitochondria reduce oxygen to water through ETC for adenosine triphosphate (ATP) synthesis. Mitochondrial respiration is the set of metabolic reactions and processes requiring oxygen that takes place in mitochondria to convert the energy stored in macronutrients to ATP, the universal energy donor in the cell. However, approximately 1-3 % of all electrons involved in this chain reaction may leak from the system, reducing oxygen to superoxide. This explains, why mitochondria are believed to be the major site of superoxide free-radical formation in the body. NAD(P)H oxidase in macrophages, leukocytes and monocytes mediates the conversion of oxygen to superoxide upon phagocytosis (Birben *et al.,* 2012). In turn, superoxide is converted into hydrogen peroxide by superoxide dismutase enzyme. Because H_2O_2 is a lipophilic molecule, it can easily diffuse through cell membrane, thus having more deleterious effect on living cells compared to superoxide (Birben *et al.,* 2012).

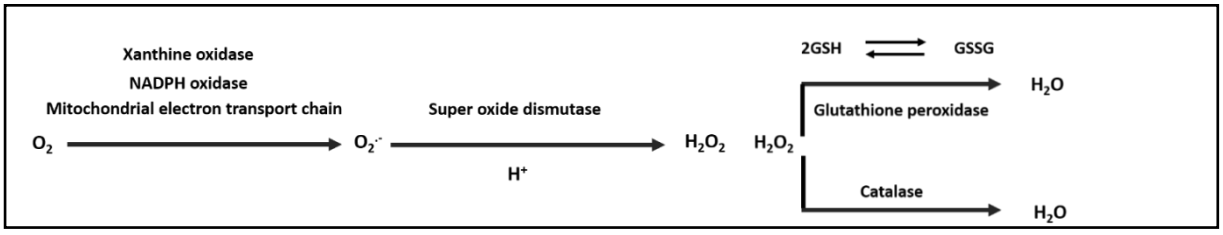

Figure 1: ROS production pathways (Lagouge and Larsson, 2003).

Iron and copper metals have high importance in biological systems by getting involved in molecular oxygen reduction. Figure 2 shows the reduction of hydrogen peroxide into hydroxyl radical by ferrous ion, known as the Fenton reaction. As show in Figure 1, reaction (2) mediates the oxidation of superoxide into molecular oxygen by ferric ion. The net balance of the reactions (1) and (2) gives Haber-Weiss reaction. Haber-Weiss reaction depicts the catalytic involvement of metal ions in the hydroxyl radical formation within the biological systems (Kanti Das *et al.,* 2014).

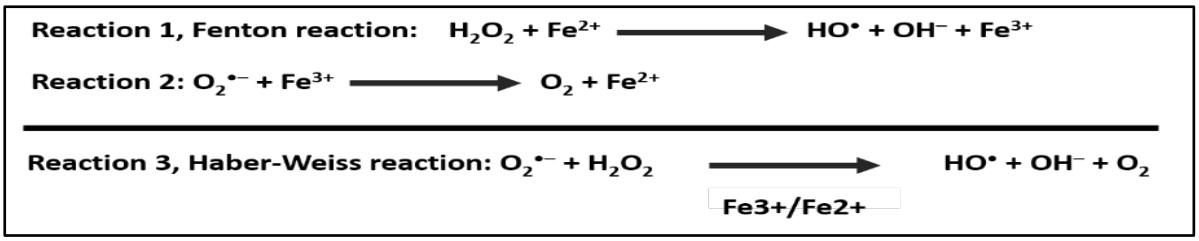

Figure 2: Hydroxyl radical formation in the biological systems (Kanti Das *et al.,* 2014).

When it comes to body physiology, no enzymatic system has been detected to neutralize hydroxyl radical, as it is very reactive within its short life period. To avoid any hydroxyl radical mediated injury of the sort of cell membrane damage, destruction of sugar groups and DNA bases sequence leading to cell death or mutation, its production must be prevented in the first step (Lushchak and Semchyshy, 2012). Amongst all free-radicals, hydroperoxyl (HOO^{-}) is the simplest one playing a significant role in fatty acid peroxidation. Myeloperoxidase is a sort of hem protein converting hydrogen peroxide to hypochlorous acid in the presence of chloride. It is commonly found in neutrophils, explaining its high anti-bactericidal potential (Santo *et al.,* 2016).

RNS generation within the biological systems

The main RNS is known to be nitric oxide (NO) that can be produced endogenously by the conversion of L-arginine amino acid by nitric oxide synthetase (NOS). NO is commonly found in the body, having a significant role in various physiological process, including neurotransmission in central nervous system, smooth muscle relaxation, immune regulation and defence mechanisms. Three types of NOS are present in body. Endothelial NOS (eNOS), expressed in endothelial cells, neuronal NOS (nNOS), mainly expressed in neurons and inducible NOS (iNOS), that is expressed in macrophages upon the release of pro-inflammatory cytokines. eNOS and nNOS are known to be produced whenever needed, thus will disappear second to minutes after enzyme activation. However, iNOS when expressed keeps on producing NO for hours to days and may harm cells (Santo *et al.,* 2016*)*. This excessive NO reacts with superoxide, generating a secondary reactive nitrogen species named peroxynitrite (Gupta, 2015). Although NO is a strong oxidant, it can only react with very specific molecules, in other words NO is a very selective oxidant. On the other hand, peroxynitrite can pass through the cell membrane reach other cells around and react with more vital biomolecules like DNA, proteins and lipids, causing DNA fragmentation, oxidative cleavage of the polypeptide backbone of the proteins, oxidation of the amino acid residue of the

side chain of proteins, generation of protein-protein cross-linkage, and lipid oxidation or peroxidation (Gupta, 2015).

Oxidative stress

Oxidants can affect biological systems in many ways, all of which are dependent on the interaction ability of oxidants with cellular components and the type of oxidants involved. Oxidants in an optimum level are essential molecules in intracellular and intercellular signalling pathways or as a defence mechanism against infections (Poli *et al.,* 2012). Various researches have proven the ability of phagocytes such as, macrophage and neutrophils to generate ROS to kill bacteria. Upon phagocytosis activation, a rapid intake of oxygen, up to 50 times more than normal, by the phagocyte occurs followed by NADPH oxidase stimulation which in turn increases the ROS production in the phagocytes as well (Santo *et al.,* 2016). On the other hand, in a healthy individual some antioxidant systems are present in the body to keep oxidant level in between an acceptable range with a balance between oxidants and antioxidants. If under any circumstances, ROS level exceeds from the predetermined range, in a way that antioxidant system cannot neutralize them, this balance is disturbed in favour of free-radicals, and an oxidative stress state is attained. Various factors may lead to oxidative stress such as suppression of the antioxidant systems or elevated levels of oxidants (Lushchak and Semchyshyn, 2012). Oxidative stress is defined as: "transient or chronic increase in steady-state level of ROS, disturbing cellular core and signalling processes, including ROS-provided ones, leading to oxidative modification of cellular constituents up to the final deleterious effects" (Ďuračková, 2010). Cells under oxidative stress, may respond to this crisis either by adapting to it or by undergoing oxidative damage depending on the intensity of the situation. Generally, cells respond to mild oxidative stress by adaptation, through the elevation of antioxidant production. A serious elevation of oxidant level can induce cell damage, known as oxidative damage by the reaction of free-radicals with important biological molecules like DNA, proteins and lipids in cell membrane, eventually causing dysfunction (Santo *et al.,* 2016).

Antioxidant classification

Antioxidants are key agents in inhibiting oxidative-stress related diseases. For instance, various researches have proven the benefit of plant derived antioxidants in preventing degenerative diseases with an oxidative-stress origin, such as; cancer, Parkinson, Alzheimer and atherosclerosis (Alagumanivasagam *et al.,* 2012). There are different attributes to classify the antioxidants.

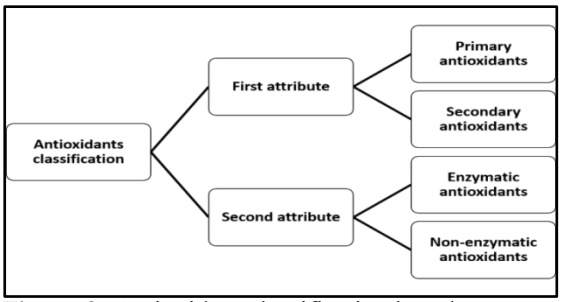

Figure 3: Antioxidant classification based on two different attributes.

The first attribute is based on the function and classifies antioxidants into the primary and secondary groups. The second attribute is based on enzymatic and non-enzymatic antioxidants (Moharram and Youssef, 2015).

Primary antioxidants (enzymatic antioxidants)

Primary antioxidants also known as enzymatic antioxidants react with lipid radicals converting them to more stable molecules, thus inhibiting the progression of chain reaction (Moharram and Youssef, 2015). These antioxidants are produced endogenously as a natural defence against free-radicals. Three main primary antioxidants present in biological systems acting synergistically and complementarily are the first line of defence against ROS known as, superoxide dismutase (SOD), catalase (CAT) and glutathione peroxidase (GPx) (Bland, 1995). Three types of SOD enzyme have been categorized based on the metal ion found in their neighbour. SOD-1 is a metalloprotein bound to copper and zinc ions localized in the cell's cytosol. SOD-2 is normally found in the mitochondria in association with manganese or iron ions. Lastly, SOD-3 is abundant in the extracellular matrix found close to copper and zinc (Aguilar *et al.,* 2016). As shown in Figure 4 (b) all of these three enzymes mediate the conversion of superoxide into hydrogen peroxide and molecular oxygen (Santo *et al.,* 2016).

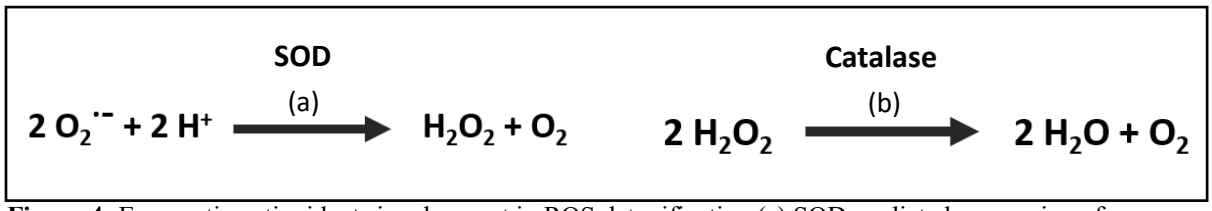

Figure 4: Enzymatic antioxidants involvement in ROS detoxification (a) SOD mediated conversion of superoxide to H_2O_2 (b) Subsequent detoxification of H_2O_2 to water and oxygen.

Catalase is an enzyme which is more or less specific to peroxisome, mediating the conversion of hydrogen peroxide to water and molecular oxygen, as shown in Figure 4 (b). Therefore, it inhibits the accumulation of hydrogen peroxide, thus preventing its involvement in Fenton reaction which normally leads to new free-radical formation (Santo *et al.,* 2016).

Glutathione systems involves the reduced form of glutathione (GSH). GSH is synthesized from glutamate, cysteine and glycine amino acids by two catalytic enzymes called, as γ-glutamylcysteine

ligase (GCL) and GSH synthetase. GSH can scavenge free radicals by direct and indirect enzymatic reactions. In the reaction of such kind, GSH is oxidized to glutathione disulphide (GSSG). Interestingly, glutathione can be recycled from GSSG by glutathione reductase enzyme. Nowadays, the antioxidant capacity of the cells is determined by the GSH/GSSG ratio which is supposed to vary between 10:1 under normal conditions. Glutathione peroxidase (GPx) are a group of enzymes with peroxidase activity. GPx enzymes use glutathione as a reductant agent to mediate reduction of hydrogen peroxide (Chaudière and Ferrari-Iliou, 1999).

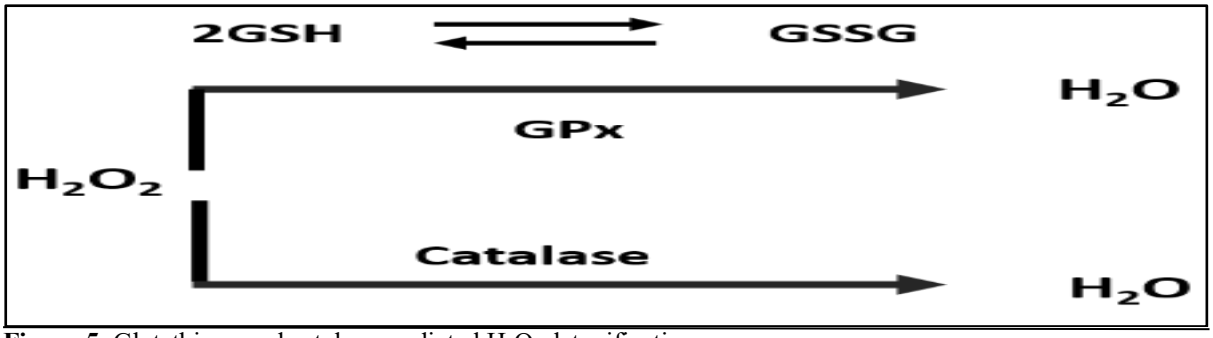

Figure 5: Glutathione and catalase mediated H_2O_2 detoxification.

Secondary antioxidants - non-enzymatic antioxidants

The non-enzymatic antioxidants, also known as secondary antioxidants, are classified into two groups: Endogenous and exogenous. Non-enzymatic endogenous system act as a second line of defence against free-radicals with the enzymatic antioxidants. These non-enzymatic endogenous antioxidants include; Thiols (glutathione, lipoic acid, N-acetyl cysteine), L-arginine, NADPH and NADH, ubiquinone (coenzyme Q10), melatonin, uric acid, bilirubin, metal binding proteins, albumin (copper), ceruloplasmin (copper), metallothionein (copper), ferritin (iron), myoglobin (iron) and transferrin (iron) (Bunaciu *et al.,* 2012). Various classes of non-enzymatic exogenous sources have been suggested amongst which polyphenols are the most important group. Polyphenol group is sub-classified to phenolic acids and flavonoids. Other classes are, vitamins, carotenoids, organosulfur and minerals (Moharram and Youssef, 2015). In vitamin group, vitamin E and C have been reported as antioxidants. Vitamin C cannot be produced endogenously, restricting its source to vegetable and fruits. Vitamin C is known to induce strong antioxidant activity on superoxide, hydroxyl and peroxynitrite radicals by donating them an electron. In contrast with vitamin C, vitamin E is lipophilic, thus playing a great protective effect on cell membrane by inhibiting lipid

peroxidation progression (Bouayed and Bohn, 2010).

Primary antioxidant VS secondary antioxidants

Primary antioxidants have the ability to scavenge millions of free-radicals. Despite primary antioxidants, secondary antioxidants can scavenge only one free-radicals. Meaning that, secondary antioxidants lose their effectivity sooner than primary ones (All antioxidants are not equivalent, 2016).

REFERENCES

Aguilar TAF, Navarro BCH, Pérez JAM (2016). Endogenous Antioxidants: A Review of their Role in Oxidative Stress, in: A Master Regulator of Oxidative Stress - The Transcription Factor Nrf2. Jose Antonio Morales-Gonzalez, Angel Morales-Gonzalez and Eduardo Osiris Madrigal-Santillan, IntechOpen.

Alagumanivasagam G, Pasupathy R, Kottaimuthu A, Manavalan R (2012).A Review on in-vitro antioxidant methods. *IJPCS.* **1**(2): 662-674.

All antioxidants are not equivalent (2016). http://bionov.fr/en/sod-b/primary-antioxidants/Accessed 13.11.2019.

Badarinath AV, Rao KM, Madhu C, Chetty S, Ramkanth S, Rajan TVS, Gnanaprakash K (2010). A Review on in-vitro antioxidant methods: comparisions, correlations and considerations. *Int J Pharm Tech Res.* **2**(2): 1276-1285.

Birben E, Sahiner UM, Sackesen C, Erzurum S, Kalayci O (2012). Oxidative stress and antioxidant defense. *World Allergy Organ J*. **5**(1): 9-19.

Bland J (1995). Oxidants and antioxidants in clinical medicine: Past, present and future potential. *J Nutr Environ Med.* **5**(3): 255-280.

Bouayed J, Bohn T (2010). Exogenous antioxidants - double-edged swords in cellular redox state: Health beneficial effects at physiologic doses versus deleterious effects at high doses. *Oxid Med Cell Longev.* **3**(4): 228-37.

Bunaciu AA, Aboul-Enein HY, Fleschin S (2012). FTIR spectrophotometric methods used for antioxidant activity assay in medicinal plants. *Appl Spectrosc Rev.* **47**(4): 245-255.

Chaudière J, Ferrari-Iliou R (1999). Intracellular antioxidants: From chemical to biochemical mechanisms. *Food Chem Toxicol.* **37**(9-10): 949-62.

Dontha S (2016). A review on antioxidant methods. *Asian J Pharm Clin Res.* **9**(8): 14-32.

Ďuračková Z (2010). Some current insights into oxidative stress. *Physiol Res.* **59**(4): 459-69.

Gupta D (2015). Methods for determination of antioxidant capacity: A review. *Int J Pharm Sci Res.* **6**(62): 546-566.

Lushchak IV, Semchyshy MH (2012). Introductory Chapter, in: Oxidative Stress - Molecular Mechanisms and Biological Effects. InTech. https://doi.org/10.5772/39292

Kanti Das T, Wati MR, Fatima-Shad K (2014). Oxidative stress gated by fenton and haber weiss reactions and its association with alzheimer's disease. *Arch Neurosci.* **2**(2): e60038.

Lagouge M, Larsson NG (2013). The role of mitochondrial DNA mutations and free radicals in disease and ageing. *J Intern Med.* **273**(6): 529-43.

Moharram HA , Youssef M (2015). Methods for determining the antioxidant activity: a review. *J Food Sci Techno.*

11: 31-42.

Phaniendra A, Jestadi DB, Periyasamy L (2015). Free radicals: Properties, sources, targets, and their implication in various diseases. *Indian J Clin Biochem.* **30**(1): 11-26.

Poli G, Leonarduzzi G, Biasi F, Chiarpotto E (2012). Oxidative stress and cell signalling. *Curr Med Chem.* **11**(9): 1163-82.

Santo A, Zhu H, Li YR (2016). Free radicals: From health to disease. *React Oxyg Species.* **2**(4): 245–263.

Tiwari K (2004). Antioxidants: New-generation therapeutic base for treatment of polygenic disorders. *Current Science.* **86**(8): 1092-1102.

www.emu.edu.tr

ISSN: 2651 - 3587

26513587022

Tasarım ve Baskı: DAÜ Basımevi, Kapak Grafik: Gizem Seracı (01.2021) T.No: ???